Research Square

Preprints are preliminary reports that have not undergone peer review.
They should not be considered conclusive, used to inform clinical practice,
or referenced by the media as validated information.

Identification and validation of WsMYB34 transcription factor for salt tolerance and induced secondary metabolism in Withania somnifera

Lakee Sharma
Banaras Hindu University
Bipin Maurya
Banaras Hindu University
Saurabh Pandey
Indian Institute of Technology Delhi
Krishna Kumar Rai
Banaras Hindu University
Shashi Pandey Pandey-Rai (shashi.bhubotany@gmail.com)
Banaras Hindu University https://orcid.org/0000-0002-6998-1594

Research Article

Keywords: WsMYB34, Salt stress, promoter binding, Withaferin A, flavonoid, CYP85A69

Posted Date: May 31st, 2022

DOI: https://doi.org/10.21203/rs.3.rs-1664631/v1

License: This work is licensed under a Creative Commons Attribution 4.0 International License.
Read Full License

Abstract

In the present study, we have identified a R2R3 type MYB protein from *Withania somnifera*, i.e., MYB34 (*WsMYB34*), known for plant development and stress tolerance. MYB transcription factors (MYB TF) have been widely implicated in conferring biotic and abiotic stress tolerance in medicinal plants. To validate this notion, we have analyzed the impact of different concentrations of NaCl on *Withania somnifera* and the potential of MYB protein in affecting the growth and development by acting as TFs in regulating the expression of defence-related genes and secondary metabolites. Since structural and functional characteristics of MYB TF in *W. somnifera* remains largely unknown, *in-silico* analysis was exploited to understand conserved binding motifs, phylogeny, 3-D structure, and role in regulating stress-responsive genes. Based on the domain analysis and phylogenetic assessment, WsMYB34 was found to be a R2R3 type MYB protein, which is phylogenetically closer to *Solanum pennellii.* In addition, interaction analysis depicted the binding capacity of WsMYB34 protein on the promoter region of a triterpenoid synthesising gene *viz; CYP85A69* (having CAACTG *cis*-regulatory sequence). The comparative microarray analysis also offered the role of WsMYB34 in abiotic stress tolerance. Exposure to NaCl imposed increased withanolide and flavonoid contents and significantly up-regulated the expression of key genes for withanolide and *WsMYB34* gene by 0.93–3.68 fold 2.61–3.47 fold respectively. The *CYP85A9* gene was also induced by 3.47 fold at 150mM NaCl. In addition, NaCl also affected growth and biochemical behaviour of *W. somnifera*. Thus, these findings depicted the role of WsMYB34 protein in plant salt tolerance.

1. Introduction

The transcription factors (TFs) are the conserved protein that controls the rate of transcription of genes by binding to a specific DNA sequence. The role of TFs in regulation of secondary metabolic and defence related genes in abiotic stress is thoroughly studied in many plants. However, a thorough study of salinity-induced adaptations in *W. somnifera* related to its secondary metabolism is untouched, especially under the regulation of transcription factors (TFs). The transcription factors are the fundamental entities of such pathways as they provide alleviation strategies to the plants. Amongst various TFs in plants, MYB, MYC, NAC, DREB, WD-40, WRKY, bZIP, ERF, etc. are the principal one to articulate genes related to secondary metabolism in a multitudinous way (Singh et al. 2002; Nakashima et al. 2012; Alves et al. 2014). Some TFs belong to highly conserved protein families in plants and are ubiquitous in all eukaryotes (Alves et al. 2014). One such protein is the MYB family, identified first as a product of animals' c-MYB (myeloblastosis-related proteins). All the TFs of this family harbour highly conserved DNA binding motifs, i.e., MYB domains (SANT regions), involved in the plant morphogenesis and stress responses (Jin and Martin 1999). Till now, four classes of MYB proteins have been identified that are categorized into different groups depending upon the presence of conserved repeats, i.e., 1R-MYB, 2R-MYB (R2R3), 3R-MYB (R0R1R2), and 4R-MYB (R0R1R2R3).The "R" repeats are DNA binding domains conserved helix-turn-helix and contain regularly spaced tryptophan (Try/W) residues. The presence of R2R3-type MYB TFs usually dominates plants that's N-terminus is highly conserved and responsible for the binding with DNA.

However, the C- terminus is highly variable and works as a trans-acting regulatory domain and for structural and functional variation in protein (Butt et al. 2017). Various reports deal with MYB TFs in plants stress tolerance like drought and salt alleviation in Rice (Tang et al. 2019) and *Arabidopsis* (Butt et al. 2017). According to Xu et al. (2017), MYB is responsible for enhanced biosynthesis of anthocyanin in carrots. However, the MYB31 gene of banana reduces the polyphenol content (Tak et al. 2017). Similarly, in Spearmint, MYB negatively regulates monoterpene production (Amarr et al. 2017).Thus; there is a need for more research to understand the regulatory mechanism of MYB TF in plant stress tolerance. In *W. somnifera*, medicinal solanaceous plant containing triterpenoidal withaferins and withanolides, we identified R2R3-type MYB *viz;* WsMYB34. In *W. somnifera*, role of comprehensive numbers of TFs has been extensively studied in plant secondary metabolism under stressed conditions. Literature is available for TFs of *W. somnifera* like WRKY and WsMYC2 under the influence of phytohormone (salicin) and jasmonic acid, respectively (Singh et al. 2017; Sharma et al. 2019). However, there is no information regarding the identification, characterization, structure prediction, and role of MYB in secondary metabolism in *W. somnifera*. Being sessile, plants have evolved many mechanisms to sense and cope with the unfavorable and successively changing environment. Plants survive in a ream of stresses like pathogen attack (biotic factors) and light, salt, radiation, drought, heavy metal, phytohormones etc. (abiotic factors) (Maurya et al. 2019; Rai et al. 2019; Apoorva et al. 2021). Under the natural environment, these stresses work together in a highly complex manner, so we cannot separate the exact impact of individual stress on plants. That's why *in-vitro* techniques are practiced to determine the actual implications of an individual and group of stresses. After the drought, salinity is the second significant constraint limiting plant growth and reproduction (Zhu 2002). Reports have also indicated that about 800 million hectares, i.e., more than 6% of global land, will deteriorate due to increasing land salinization (Munns and Tester 2008). Plants in saline conditions, especially under NaCl (the most widely distributed soluble salt), show significant osmotic imbalances, cell death, declined pigmentation, increased secondary metabolism, and antioxidative defense system (Greenway and Munns 1980; Zhu 2002; Parida and Das 2005). In *Withania somnifera* (Ashwagandha) salinity causes increased antioxidative defence system and withanolide production up to mild concentration (Sabir et al. 2012). Therefore, the present study can help to the role of MYB TF in salinity-induced alterations and secondary metabolism in *W. somnifera*. In this study, the primary considerations were taken, (1) to identify and characterize the novel WsMYB34 protein, (2) to investigate the binding analysis of WsMYB34 with promoter of triterpenoid synthesising gene i.e. *CYP85A69* using bioinformatics tools, (3) to determine the expression level of *WsMYB34* and different essential genes of withanolide production under salt stress. In addition to this, this study aims to elucidate the effect of NaCl on growth and biochemical behaviour of *W. somnifera*.

2. Material And Methods

2.1 Database search for nucleotide sequences of WsMYB34 and phylogenetic analysis

We have performed the Illumina sequencing from PCR based subtractive hybridization, using cDNA population derived from *W. somnifera* leaf mRNA which was translated by ExPASy translation tool https://web.expasy.org/translate/. Further, identification and nomenclature of the protein was performed by Pfam and BLAST-TAIR tools respectively. The sequence annotation was done by BLASTp server. Phylogenetic tree of WsMYB34 protein sequence among all homologues was constructed by N-J method of MEGA version 4.0.02 (Tamura et al. 2013). Each node was tested using the bootstrap approach by taking 1,000 replications. This observation was dependent on the results of phylogenetic clustering by using Clustal W https://www.ebi.ac.uk/Tools/msa/clustalo in the form of percentage similarity matrices (Larkin et al. 2007).

2.2 Domain analysis of WsMYB34 protein

Functional R2R3 domains in the form of two SANT protein regions were identified by using different domain identification tools like PROSITE, SMART, SWISS-PROT, Pfam, NCBI CDD server, and InteProScan. The distribution and arrangement of conserved motifs in WsMYB34 protein were identified with the help of MEME Suite 4.1.1.2 http://meme.ncbr.net (Bailey et al. 2006).

2.3 Structural modelling and model validation of WsMYB34 protein

The protein sequence of WsMYB34 was taken further for homology modelling and DNA- protein docking analyses. Identification of structurally resolved templates similar to WsMYB34 was made by SWISS-MODEL https://swissmodel.expasy.org/ and I-TASSER tools (Waterhouse et al. 2018). The SWISS Modeller tool selected the four most identical protein templates to generate the refined 3-D structure of a protein. The templates were the crystal structure of transcription factor WER (PDB ID: 6KKS), the design of the *Trichomonas vaginalis* Myb3 DNA-binding domain (PDB ID: 3zqc), the crystal structure of ternary protein- DNA complex3 (PDB ID: 1h8a), and NMR resolved structure of Chicken B-MYB DNA binding domain (PDB ID: 1a5j). Further refinement at the atomic level was done by the refinement tool ModRefiner (Xu and Zhang 2011). The model topology and other surface features were assessed by superimposing it with each of the templates using Superpose version 1.0 (Maiti et al. 2004), and alignment between WsMYB34 and templates was performed using the MultAlin online tool http://multalin.toulouse.inra.fr/multalin/multalin.html. The accuracy and reliability of the model were compared with resolved templates on different qualitative and quantitative parameters. Various single model methods were used for quality prediction, such as ERRAT http://services.mbi.ucla.edu/ERRAT/stats/ (Colovos C. and Yeates T. 1993) and ProSA https://prosa.services.came.sbg.ac.at/ (Wiederstein et al. 2007). For quantitative assessment, the VADAR tool http://vadar.wishartlab.com/analysis was used (Willard et al. 2003). Confirmation of the predicted model was inspected by Ramachandran plot using the PROCHECK module of the PDBsum server http://www.ebi.ac.uk/pdbsum/ (Laskowski 2009). The 3D profile of the expected model and templates was done by verify- 3D server. To retrieve the accession identities, the final validated model was submitted in PMDB (protein modelling database) https://bioinformatics.cineca.it/PMDB/ (Castrignano et al. 2006).

2.4 Structure- based functional annotation

Functional annotation (in biological terms), based on the structure of modelled protein WsMYB34, was done by COFACTOR server (Roy et al. 2012). The CATH server performed further structural classification and functional classifications of identified superfamilies were performed using FunFHMMer http://www.cathdb.info/search/byfunfhmmer. These results were further analyzed using gene ontological terms (Das et al. 2016). The GO terms distribution test analysis was conducted using the REVIGO server http://revigo.irb.hr/ (Supek et al. 2011).

2.5 Active site prediction and sub-cellular localization

Active site and involved residues in ligand binding with WsMYB34 were predicted by Metapocket 2.0 http://metapocket.eml.org/. To detect the sub-cellular localization of query protein, it was subjected to submit in various online servers like CELLO2GO (subCELlular LOcalization prediction) http://cello.life.nctu.edu.tw/cello2go/ (Yu et al. 2014).

2.6 WsMYB34 protein and *CYP85A69* promoter binding analysis

To attest the role of MYB TF in regulation of secondary metabolism, the MYB binding *cis*-regulatory elements of promoter of triterpenoid synthesising gene of *W. somnifera* i.e. *CYP85A69* (Accession no.- MK611931) were identified by PlantCare tool. The results attested the presence of CAACTG regulatory DNA sequence in the promoter which was further docked with WsMYB34 protein by Patchdock molecular docking server (Schneidman-Duhovny 2005) and the resultant docked complex was observed by Discovery studio 3.0.

2.7 Plant materials and salinity treatment

Seeds of *Withania somnifera* were sown in autoclaved sand and soil. Seedlings at four-leaf stage were transferred in half strength Hoagland solution (Hoagland and Arnon 1950). For salinity treatment 5 weeks old plantlets were initially divided in 6 groups. The 1st group taken as control (without NaCl) while plantlets of 2nd to 6th groups were transferred in half strength Hoagland solution supplemented with 50, 100, 150, 200, and 250mM NaCl, respectively, for a week under 18 hours light and 25 ± 2°C temperature.

2.8 Analysis of secondary metabolism of *Withania somnifera*

Analysis of Withaferin A was performed by HPLC. Sample preparation was done according to Tripathi et al. (2021). Filtered samples were run in an isocratic reverse C-18 column HPLC system equipped with a 2707 autosampler 515 HPLC pump assembled on 2998 PDA detector and the flow rate was l ml min^{-1}. The mobile phase was acetonitrile: water (45: 55) with 0.1% acetic acid (Sharma 2013). Estimation of total flavonoid content was done by following the spectrophotometric method of Chang et al. (2002) and calculated using standard curve of quercetin. Chromatographic and spectrophotometric analysis was

validated by expression profiling of respective genes. RNA was extracted by TRIZOL reagent (GIBCO-BRL) and purity and quantity of isolated RNA was assessed on Nano Drop (Thermo scientific) by taking the absorbance at 260/280 nm. The synthesis of cDNA was carried out by RNA in MyCycler according to the manufacturer's instructions. Primers for withanolide and flavonoid synthesizing genes and *WsMYB34* were designed by employing Primer 3 software (Table S1). Analysis of gene expression level have been carried by semi-quantitative RT-PCR using thermo cycler and band intensities were quantified by running the product on 2% agarose gel and observing under GelDOC EZ imager (Bio-Rad). Real-time PCR was performed by the CFX-96 system of Bio-Rad and for normalizing the transcript levels; *RPS9* was used as an endogenous gene. The amplification results were calculated by comparative threshold cycles (2-ΔΔ Ct method). Amplification of primer was identified by melting curves.

2.9 Comparison of expression pattern of *WsMYB34* with model plants

In the form of their transcriptional profiles, the available expression data of MYB genes from the model plants were compared with the expression pattern of the WsMYB34 gene. The expression data of two model plants, i.e., Arabidopsis and Rice were collected from AtGenExpress Visualization Tool (http://jsp.weigelworld.org/expviz/expviz.jsp) and AffymetrixGeneChip rice genome arrays (HTTP://www.ncbi.nlm.nih.gov/geo/) respectively and the expression profiles were determined.

2.10 Estimation of plant growth parameters and photosynthetic attributes

For experimentation, three plants were taken from each set. Fresh weight (FW) and dry weight (DW) of NaCl untreated and treated plants were taken on digital balance (BL60S, Sartorious). Relative water content (RWC), FW, DW, and turgid weight (TW) of leaves were recorded and calculated according to (González and González-Vilar 2001). Estimation of Chl. a, Chl. b and carotenoid were done according to the Porra et al. (1989) and for measurement of Anthocyanin content protocol of Mancinelli et al. (1975) was followed to evaluate chlorophyll fluorescence, plants were kept under dark condition for 20 min. Minimum fluorescence (F_0) and maximum florescence (Fm) were recorded with the help of portable chlorophyll fluorometer (PAM-2500). Variable fluorescence (Fv) has been deduced from F_0 andFm and finally the value of Fv/ Fm was derived.

2.11 Estimation of biochemical parameters

The total content of phenolics were estimated by Folin- ciocaulteu assay and calculated as catechol equivalents from a standard curve (Imeh and Khokhar 2002). For proline estimation, we used the method described by Bates et al. (1973). Total protein content was recorded according to Lowry et al. (1951) and was calculated from the known concentration of BSA. For estimation of total soluble sugar method given by McCready et al. (1950) was used.

2.12 Determination of MDA content and DPPH activity

Lipid peroxidation (LPO) was determined by measuring malondialdehyde (MDA) in the form of TBARS content using extinction coefficient 155 mM^{-1} cm^{-1} (Heath and Packer 1968). For free radical scavenging activity, percent inhibition of DPPH activity was measured by formula-

DPPH % Inhibition= (A0-A1)/A0×100

Where, A0 = the absorbance of control, A1 = the absorbance of sample.

2.13 Fluorescent microscopy of trichomes and analysis of stem anatomy

Fluorescence microscopy of *W. somnifera* from leaf samples have been carried out according to Munien et al. (2015). Leaves were first stained in Rhodamine B, washed, and observed under fluorescent microscope at 550/582 nm wavelength (excitation/ emission) respectively. Fine handpicked stem sections were dehydrated using a series of alcohol dilutions followed by washing (30, 50, 70, 90, and 100% each for 5 min) and observed under a Dewinter image microscope.

2.14 In-vivo determination of ROS and cell death by staining of leaves

The content of H_2O_2 and $O_2^{\bullet-}$ generation was determined by dipping the leaves in 3, 3'-diaminobenzidine (DAB) and nitroblue tetrazolium (NBT) solutions respectively (Thordal- Christensen et al. 1997; Frahry and Schopfer 1998) and the extent of cell death in leaves induced by salinity was observed by staining with Evans Blue. Leaves were dipped in 0.025% m/v Evans blue in 100 µM $CaCl_2$ (pH 5.6) then washed properly and observed.

2.15 Statistical analysis

All the experiments were performed in three biological replications and subjected to ANOVA. The mean differences were compared by performing Duncan's multiple range test (DMRT) using SPSS software (SPSS Inc., Version 20.0) and values at $P \leq 0.05$ were considered significant. All the graphical presentations of the data were plotted on Sigma plot software (version 11.0). The significant positive and negative correlations between control and each NaCl treated plant sets were performed after calculating the correlation coefficient (*r*).

3. Results

3.1 Data retrieval and comparative phylogenetic and motif analysis

The discovered nucleotide sequence of MYB TF of *Withania somnifera* was submitted in NCBI GenBank (accession number- OK484488). The phylogenetic analysis of WsMYB34 across all plant species homologs, including monocots and dicots, divided the candidate protein in two groups i.e., cluster A and B. This indicates that this protein gene family is strictly conserved and has evolved from ancestral plants

(Fig. 1a and 1b). Tree analysis revealed the closest resemblance of WsMYB34 with *Solanum pennellii* MYB15 (XP_015081791), *Capsicum baccatum* MYB34 (PHT43364), *C. chinense* MYB34 (PHU12253) (Fig. 1a). Further, the Phylogenetic analysis by taking monocot and dicot model plants i.e., Rice and Arabidopsis respectively also showed the similarity of WsMYB34 with stress responsive MYB proteins (Fig. 1b). This type of highly conserved nature of such proteins plays important role in plant stress responses and secondary metabolism. The R2 and R3 domains were observed by I-TASSER tool which showed highest sequence conservation at the N-terminus of WsMYB34 protein (Fig. S1). The distribution of motifs in all members of MYB proteins was performed statistically, in terms of their *E*- and *p*- values which represent how frequently each motif is distributed and what is the probability of their individual occurrence, respectively. Our result represents distribution of highly conserved and evenly distributed motifs at N- terminus while variability was observed at C- terminus of MYB proteins. R2 and R3 domains of MYB protein constituted by 4 motifs i.e. motif 4 (TWTPEEDRKLAAYITKYGS; *p*- value 2.22e-14, and *E*- value 1.6e-171), and motif 1 (WNWRQLPKYAGLARCGKSCRLRWMNYLRPN; *p*- value 3.48e-40, and *E*- value 4.1e-342) formed R2 domain, however, R3 domain was covered by motif 7 (VKRGNYTKEEDEII; *p*- value 1.93e-17, and *E*- value 3.0e-123) and motif 2 (LHAQLGNKWSAIAAHLPGRSDNEIKNHWHT; *p*- value 4.03e-38, and *E*- value 2.0e-316) (Fig. 1c).

3.2 Domain analysis

Analysis of the presence of conserved domains in WsMYB34 was cumulatively performed by the InterProScan tool that retrieves the results from Pfam, SMART, NCBI CDD, and PROSITE profiles (Fig. S2, S3, and S4). Results revealed the occupation of the MYB/SANT domain, from 2nd to 97th amino acid residue and two MYB-DNA-binding domains (stretching from 11th to 44th and 50th to 94th amino acids respectively). These conserved domains were found to be located on the N-terminus of our protein, which evidenced the conserved nature of the first half and variable nature of the second half of the MYB protein. Both the R2 and R3 repeats in the protein contained evenly distributed and highly conserved signature amino acids, including Tryptophan (W) residues at specific intervals that were located on 1st, 21st, and 41st positions in R2 domain while in the R3 repeat, it was on 54th, 73rd (substituted with phenylalanine), and 92nd positions (Fig. S1). These core sequences are the landmarks in DNA binding domain (DBD) of plant MYB proteins. Despite the signature domains, DNA binding sites were also observed by the CDD server, as Arg^{31}, Cys^{32}, Lys^{34}, Ser^{35}, Arg^{37}, Leu^{38}, Arg^{39}, Met^{41}, Asn^{42}, and Tyr^{43} were found to be involved in binding with target DNA. These residues were lying within the range of MYB domain.

3.3 Structural modeling and model validation

The most appropriate and experimentally resolved templates for WsMYB34 protein were chosen from SWISS-MODEL and I-TASSER tools. The template named 6kks.1.A, having most significant hit was used for protein homology modeling. The 3-D model of our protein was finally generated by using SWISS Modeller server. The model satisfying maximum validation parameters was refined further and final model was submitted to PMDB with a unique ID (PM0084118) (Fig. S5). In the present study, N- terminal domain for WsMYB34 was modeled and found to satisfy all the electrostatic parameters that are

important for reliability of computationally generated 3-D models (Fig. 2a). In this context, for DNA-protein interaction analysis, the MYB binding DNA element C/TAACG/TG3 was modeled by DNA sequence to structure conversion tool (Fig. 2b) (http://www.scfbio-iitd.res.in/software/drugdesign/bdna.jsp). The VADAR produced the topological assessment of our modelled protein by performing homology modelling and 3-D threading. Topological conformations for WsMYB34 protein were attested to have helix type secondary structure, containing 68 (62%) helix, 7 (6%) beta, 34 (31%) coil, and turns 16 (14%). While, 95 (87%) residues were found with H bond, having observed H bond mean energy (-1.5, SD = 1.1) against the expected value of -2.0 (SD = 0.7). Quantitative assessment of the modelled protein (before and after refinement) was checked for Ramachandran plot analysis, which was performed by RAMPAGE server, PDBsum server of PROCECK, and MolProbity algorithms. Results of the MolProbity revealed the percentages of amino acid residues of proteins in favoured and allowed regions to be 85.0%, and 97.2% for model before refinement and 98.1%, and 100% for model after the refinement, over expected values of 98% and > 99.8% respectively (Table S2 and Fig. S6). This pattern was also obtained by the RAMPAGE server and PROCHECK tool, which attested 98.1% residues of refined model residing in favoured region (expected 98%), 1.9% in allowed region (expected 2%), and 0% in outlier (Fig. 2c). In this study, the four templates were also analyzed along with predicted the model. Further validation was performed by quantifying ProSA, ERRAT, Verify 3D, QMEAN, and Resprox scores. Scoring by ProSA server indicated very close and less structural error gaps in predicted model, which was measured in terms of Z- score of the model and template (Fig. 2c and Table 1). Other tools like ERRAT and Verify 3D validated the higher scores of model (99%) than X- ray and NMR resolved templates. Verify 3D calculated the 3D/1D profile of predicted model and it was found to be 97.25% (more than 80% required), while values for templates were less than the values of model. Conformity for the accuracy of MYB predicted model was again authenticated by RESPROX server, which scores the model 1.88.

Table 1
Qualitative and quantitative assessment of WsMYB34 protein and its comparison with structurally resolved models

S. no.	Protein name	QMEAN score	Z-score	Overall quality (ERRAT score)	ResProx	Verify 3-D (3D/1D profile)
1	WsMYB	-1.11	-5.52	99.00	1.88	97.25%
2	6kks (crystal structure of Transcription factor WER/DNA Complex)	0.31	-6.62	93.87	1.41	83.02%
3	1h8a (Crystal structure of ternary protein- DNA complex3)	1.33	-7.28	100.00	2.07	45.83%
4	3zqc (*Trichomonas vaginalis* Myb3 DNA-binding domain)	-2.60	-1.12	78.30	3.11	79.49%
5	1a5j (NMR structure of Chicken B-MYB DNA binding domain)	-6.07	-4.76	27.45	5.01	80.66%

A good quality protein have ReSProx values ranging between 0–1.5, Errat score more than 90, minimum Z and Qmean scores with occupying more than 98% of the residues in most favoured region, less than 2% residues in additionally allowed region and 0% residues in outlier region in RAMPAGE analysis.

3.4 Superimposition results

The superimposition analysis between target WsMYB34 protein domain with its experimentally resolved templates 6kks, 1h8a, 3zqc, and 1a5j on the basis of comparative topological (structural) parameters was done by Superpose software which depicted the high similarities between WsMYB34 functional domains and templates 6kks, 1h8a, and 3zqc as compared to 1a5j (Fig. 3a). This was further confirmed by computing local as well as global RMSD values for each template and target interaction which were 1.24, 0.91, 0.77, and 1.99 A° alpha carbon for 6kks, 1h8a, 3zqc, and 1a5j respectively. The sequences of the functional domain of target protein and its four templates were aligned by the MultAlin tool that categorized the amino acid sequences in different colors, on the basis of the degree of conservation. A high consensus sequence was denoted by red, low by blue, and neutral by black. Low similarities have occurred due to synonymous and non-synonymous substitutions. In our result, the Tryptophan residues were found to be structurally highly conserved (Fig. 3b).

3.5 Analysis of Gene Ontology (GO) and enrichment: structure based function prediction

For Gene Ontology analysis, our protein sequence was assessed by the CATH server for prediction of molecular, biological, and cellular functionalities, as well as to locate the Subcellular compartments. The CATH classified WsMYB34 protein to sustain mainly alpha type structure (C- level, 1), orthogonal bundle (A- level, 1.10), Arc repressor mutant, subunit A (T- level, 1.10.10), and homeodomain- like structure (H-

level, 1.10.10.60). The ReviGO further analyzed vocabularies obtained by CATH in the form of GO terms through a scatter plot diagram (Fig. S7). In this reference, we found five significant GO terms pertaining to biological process i.e., response to- jasmonic acid (GO: 0009753), wounding stress (GO: 0009611), salt stress (GO: 0009651), UV exposure (GO: 0010224), and regulation of transcription (GO: 0006355). On the other hand, four significant terms were found under molecular processes i.e., protein binding (GO: 0005515), DNA binding (GO: 0043565), sequence specific DNA binding (GO: 0003677), and sequence specific transcription factor activity (GO: 0003700). The deduced gene ontology and results of Cello2GOwere further taken for the subcellular localization of predicted WsMYB34 protein. Results depicted that the protein mainly reside in the nucleus with 49% probability (score- 2.449), followed by in mitochondria (17.4%, score- 0.868). As shown in Fig. 4, predicted protein was assessed to mostly engage in molecular functions like DNA binding (42.5%), and chromatin binding (41.8%). Similarly, structure based functional prediction by COFACTOR server also shown the involvement of WsMYB34 protein in various cellular, molecular, and biological activities (data not shown).

3.6 Binding analysis of WsMYB protein on promoter of *CYP85A69* gene

The refined model of our WsMYB34 protein was studied so for DNA-protein interaction by docking it against the major groove of *CYP85A69* promoter having C/TAACG/TG nucleotide sequence as MYB binding site (Fig. 5). This interaction analysis was performed by choosing default parameters of the Patchdock server. The docked complex having the highest score was selected. In this context, we found the maximum score to be 9694, covering 1350.20 areas with a negative ACE value. Next, the amino acid residues, involved in DNA-protein interaction were observed and results revealed that most of the linkage was supported from the R3 domain of the modelled protein, mainly through conserved tryptophan residues (Fig. 5b and 5c).

3.7 Comparative microarray analysis of WsMYB34

The expression pattern of WsMYB34 protein was compared with the available microarray data of model plants *viz*; *Oryza* and *Arabidopsis*. The heat map of microarray-based expression pattern of MYB genes from Rice revealed that OsMYB, OsMYB30, and OsMYB2 showed high level of expression under abiotic stress in most of the tested tissue (Fig. 6a). Some other OsMYBs showed constitutive expression in developmental stages of Rice (Fig. S8a and Fig. S9a). These results suggested the role of MYB in plant development and metabolism under stress. Likewise, MYB isoforms' from Arabidopsis were also shown to highly express under different abiotic stresses like salt, drought, ABA, and chilling (Fig. 6b).

3.8 Gene expression analysis of secondary metabolic and WsMYB34 gene and estimation of Withaferin A and flavonoid

We performed a semi-quantitative RT-PCR analysis of the terpene and steroid biosynthetic genes and the WsMYB34 gene to validate the HPLC analysis. Under the exposure of NaCl treatment, expressivity of the

genes such as *HMGR, HMGS, DXS, FPPS, DWF1, DXS, SMO1, FK, HYD1*, and *SMT1* as well as *WsMYB34* were found to be up-regulated by 1.47–2.03, 1.69–3.09, 0.93–1.21, 0.98–1.07, 1.31–2.08, 1.04–1.24, 1.53–2.11, 1.02–1.41, 2.52–3.68, and 2.61–3.47 fold, respectively (Fig. 7a). However, the maximum expression level of *WsMYB34, FPPS, DWF1, DXS*, and *FK* was recorded with 150mM NaCl concentration. For clustering of different doses of NaCl in terms of the expressivity of secondary metabolite and defense-related genes, a heat map was constructed which depicted that higher doses, i.e., 200 and 250mM NaCl, form a separate cluster with control plants as compared to low concentration of NaCl treated plants (Fig. 7b). Further, Real-time PCR analysis of *WsMYB34, SMT1, XDR*, and *DWF1* genes showed maximum up-regulation under the exposure of 150mM NaCl concentration. Figure 7c clearly showed 5.6, 6.4, 8.6, and 4.2 fold over-expression of *WsMYB34, SMT1, DXR*, and *DWF1* genes with 150mM NaCl treated plants as compared to control plants. Besides this, expression analysis of flavonoid synthesizing genes (i.e. *CHS*, *CHI*, and *PAL*) and terpene-related genes i.e. *CYP83B1* and *CYP8569A*) was also induced by NaCl (Fig. S10). In this study, we have carried out chromatographical analysis of alcoholic leaf extracts obtained from salt treated as well as non- treated control plants. Since, previously it is reported that in aerial parts of *Withania somnifera* harbor higher amount of Withaferin A than Withanolide A, thus we have estimated the content of only Withaferin A (Gupta et. al 1996). As shown in Table 2, we estimated a surge in µg/g fresh weight withaferin A content from 1.12 to 1.68 fold and the maximum increase was recorded for 150mM treated plants (2.17 fold). The similar trend was also obtained when secondary metabolite content was estimated in the form of µg/g dry weight. The flavonoid content of plant was recorded to increase significantly according to increasing doses of NaCl (Table 2).

Table 2
Withaferin A and flavonoid content in various concentrations of NaCl treated and non- treated control plants of *Withania somnifera*

Treatments	Withaferin A content		Flavonoid content
	µg/gFW	µg/gDW	(mg/100g FW)
Control	28.71 ± 3.22^{c}	2.90 ± 0.32^{ab}	43.68 ± 4.96^{c}
50mM	32.42 ± 0.41^{bc}	3.42 ± 0.043^{ab}	66.48 ± 5.60^{b}
100mM	42.48 ± 2.22^{abc}	4.35 ± 0.22^{ab}	71 ± 1.3^{b}
150mM	63.45 ± 4.27^{a}	6.40 ± 0.43^{ab}	74.65 ± 3.2^{ab}
200mM	51.95 ± 11.69^{ab}	6.05 ± 0.203^{a}	95.08 ± 6.32^{a}
250mM	49.16 ± 6.34^{abc}	5.18 ± 0.94^{ab}	93.68 ± 12.50^{a}

The values of different characters (average of three replicates ± SE) in the same column with different letters in superscript are significantly different from each other by applying Duncan's multiple range test ($P < 0.05$). Data analysis was based on one-way ANOVA.

3.9 Effect of NaCl on morphological attributes and relative water content (RWC) of *Withania somnifera*

Salinity imposed a notable decrease in morphological characteristics as, maximum stem height (36.3%), fresh weight (60%), and dry weight (53.3%), total no. of leaves; nodes, leaf length, leaf width, and petiole length in plants were recorded after 150 and 200mM NaCl treatment respectively (Table 3). Salt concentration also caused a remarkable decline in the percentage of RWC of the plant leaves with a 9.1%, 18.3%, and 24.4% decrease after 150, 200, and 250mM treatments respectively.

Table 3
Effect of NaCl on morphological attributes and relative water content (RWC) of hydropically grown *Withania somifera*

Parameters	NaCl (mM concentration)					
	Control	50	100	150	200	250
Stem height (cm)	8.33 ± 1.21^{a}	7.10 ± 0.95^{ab}	6.00 ± 0.77^{ab}	5.30 ± 0.15^{b}	2.60 ± 0.20^{c}	1.76 ± 0.39^{c}
Fresh weight (g)	0.45 ± 0.04 ^{a}	0.48 ± 0.09^{a}	0.36 ± 0.03^{ab}	0.32 ± 0.09^{ab}	0.18 ± 0.02^{b}	0.17 ± 0.01^{b}
Dry weight (g)	0.045 ± 0.003^{a}	0.045 ± 0.009^{a}	0.037 ± 0.009 ^{ab}	0.032 ± 0.008^{ab}	0.021 ± 0.001 ^{b}	0.018 ± 0.002^{b}
Total no. of leaves	12.0 ± 1.0 ^{a}	11.6 ± 0.88^{a}	10.3 ± 0.66^{a}	9.0 ± 1.0^{a}	5.3 ± 0.88^{b}	3.6 ± 1.2^{b}
Total no of nodes	8.66 ± 1.41^{a}	7.66 ± 0.99^{ab}	6.86 ± 0.77^{b}	3.67 ± 0.77^{c}	3.2 ± 0.15^{c}	3.0 ± 0.11^{c}
Leaf length (cm)	3.80 ± 0.37^{a}	3.70 ± 0.32^{a}	3.20 ± 0.15^{ab}	2.83 ± 0.2^{bc}	2.06 ± 0.26^{cd}	1.73 ± 0.12^{d}
Leaf width (cm)	2.60 ± 0.17^{a}	2.53 ± 0.13^{a}	2.23 ± 0.03^{ab}	1.76 ± 0.07^{bc}	1.36 ± 0.38^{cd}	1.06 ± 0.29^{d}
Petiole length (cm)	0.93 ± 0.08 ^{a}	0.80 ± 0.05 ^{ab}	0.71 ± 0.10 ^{bc}	0.65 ± 0.05^{bc}	0.50 ± 0.01 ^{cd}	0.40 ± 0.05 ^{d}
Whole trichome length (µm)	113.71 ± 11.70^{b}	236.37 ± 17.56 ^{a}	254.67 ± 9.20 ^{a}	293.99 ± 45.08 ^{a}	266.57 ± 9.11 ^{a}	251.92 ± 16.25 ^{a}
RWC (%)	0.98 ± 0.01 ^{a}	0.94 ± 0.01 ^{ab}	0.96 ± 0.06 ^{ab}	0.89 ± 0.02 ^{b}	0.80 ± 0.03 ^{c}	0.74 ± 0.05 ^{c}

The values of different characters (average of three replicates ± SE) in the same row with different letters in superscript are significantly different from each other by applying Duncan's multiple range test ($P < 0.05$). Data analysis was based on one-way ANOVA.

3.10 Effect of salt stress on photosynthesis and biochemical parameters

We have investigated that all the salt treated plants showed lower photosynthetic efficiency than the non-treated control plants (Table 4). Significant decline in the contents of chl. a, chl. b, and total chl. were recorded after a higher dose of NaCl. Dose- dependent reduction in the carotenoid content was measured upto 14.8, 26, 35.2, 41.1, and 53.2% after 50, 100, 150, 200, and 250mM NaCl concentration respectively. However, anthocyanin levels were found to be elevated when plants were exposed to 150mM salt treatment with 1.31 fold increment as compared to control (Table 4). In case of chlorophyll florescence the decrease in Fv/Fm ratio in 250mM treated plants (0.68 i.e., 10.52% decrease) significantly varies as compared to the control (Table 4). These outcomes depicted the occurrence of photoinhibition in plants at extreme doses of NaCl. To attest the biochemical changes that have occurred under the influence of NaCl, the levels of phenol, proline, total sugar, protein, MDA (lipid peroxidation), and DPPH (free radical scavenging activity) were recorded by colorimetric methods (Table 4). Throughout this study, the accumulation of total phenolic compounds and proline content were found to be indubitably and significantly up-regulated at a rate of 69.5-257.3% and 18-71.4% respectively, in dose- dependent manner. Other biochemical activities like total sugar content, lipid peroxidation, and DPPH activity followed the same pattern with increments of 1.05–2.03, 1.33–2.2, and 1.14–1.34 folds respectively. The free radical activity was estimated to decline slightly (1.07 fold) after extreme salt exposure i.e., 250mM as compared to 200mM NaCl treatment. The significant increment of 34.65% protein content was found in the leaves of 100mM NaCl treated plants. Among the treated plants, retardation in protein accumulation was accomplished by 29.5 and 55.2% decline after extreme doses of salt i.e., 200 and 250mM NaCl respectively.

Table 4
Impact of NaCl on photosynthetic and biochemical parameters of *Withania somnifera*

Parameters	NaCl (mM concentration)					
	Control	50	100	150	200	250
Chl a (mg g^{-1} FW)	3.10 ± 0.13^{a}	2.87 ± 0.26^{ab}	2.64 ± 0.31^{abc}	2.02 ± 0.34^{bc}	1.97 ± 0.29^{bc}	1.86 ± 0.30^{c}
Chl b (mg g^{-1} FW)	1.28 ± 0.06^{a}	1.10 ± 0.071^{ab}	0.89 ± 0.038^{bc}	0.85 ± 0.031^{cd}	0.68 ± 0.124^{cd}	0.62 ± 0.077^{d}
Total chl (mg g^{-1} FW)	4.39 ± 0.18^{a}	3.97 ± 0.33^{ab}	3.53 ± 0.34^{abc}	2.88 ± 0.33^{cd}	2.65 ± 0.41^{d}	2.49 ± 0.38^{d}
Carotenoid (mg g^{-1} FW)	2.055 ± 0.14^{a}	1.758 ± .049^{ab}	1.522 ± 0.15^{bc}	1.33 ± 0.095^{bcd}	1.219 ± 0.20^{cd}	0.962 ± .053^{d}
Anthocyanin (absorbance g^{-1} FW)	0.383 ± .05619^{a}	0.484 ± .0789^{a}	0.504 ± .05325^{a}	0.477 ± .04062^{a}	0.434 ± .049^{a}	0.409 ± .035^{a}
Fv/*Fm*	0.76 ± 0.003^{a}	0.75 ± 0.03^{ab}	0.72 ± 0.024^{ab}	0.72 ± 0.029^{ab}	0.70 ± 0.014^{ab}	0.68 ± 0.006^{b}
Proline (µmole g^{-1} FW)	3.54 ± 0.065^{d}	4.18 ± 0.100^{c}	4.60 ± 0.070^{bc}	5.19 ± 0.20^{b}	5.88 ± 0.069^{a}	6.07 ± 0.430^{a}
Phenol (mg g^{-1} FW)	94.833 ± 8.14^{d}	160.79 ± 2.57^{cd}	184.41 ± 12.44^{c}	288.33 ± 6.26^{b}	309.0 ± 3.58^{b}	338.83 ± 15.98^{a}
Protein (µm g^{-1} FW)	3.54 ± 0.25^{abc}	4.72 ± 0.64^{a}	4.76 ± 1.34^{a}	3.78 ± 0.49^{ab}	2.50 ± 0.29^{bc}	1.58 ± 0.069^{c}
Sugar (µg mg^{-1} FW)	12.77 ± 1.17^{c}	12.93 ± 0.187^{c}	16.90 ± 2.58^{bc}	19.49 ± 1.35^{ab}	21.06 ± 6.48^{ab}	25.84 ± 4.48^{a}
Lipid peroxidation MDA (mm g^{-1} FW)	0.326 ± 0.045^{b}	0.436 ± 0.012^{ab}	0.539 ± 0.014^{ab}	0.701 ± 0.011^{ab}	0.606 ± 0.070^{ab}	0.520 ± 0.018^{a}
Free radical scavenging activity (% inhibition)	71.23 ± 12.20^{b}	81.38 ± 4.25^{ab}	88.83 ± 4.405^{ab}	87.64 ± 6.64^{ab}	96.05 ± 2.25^{a}	93.23 ± 3.14^{a}

The values of different characters (average of three replicates ± SE) in the same row with different letters in superscript are significantly different from each other by applying Duncan's multiple range test ($P < 0.05$). Data analysis was based on one-way ANOVA.

3.11 Effect of NaCl on leaf surface trichomes density of Withania somnifera

Fluorescent microscopic results depicted the gradual progression in the number of surface trichomes per unit area in accordance with the increasing concentration of NaCl (Fig. S11). The maximum number of non-glandular trichomes (NGT) was observed on 250mM NaCl treated plants, while the highest density of glandular trichomes (GT) was limited to 150mM treated plants. Further, with the help of ImageJ software, the length of the whole trichome as well as expanded branches of NGT was calculated. The maximum length was observed from 150mM treated leaves i.e., 293.99 and 186.44µm for whole length and height of the trichome branch respectively (Table 5). There was a 2.08, 2.24, 2.60, 2.35, 2.22 fold increase in whole trichome length as compared to control, for 50, 100, 150, 200, and 250mM NaCl plants respectively.

Table 5
Effect of NaCl on trichome length of *Withania somnifera*

Treatments	Withaferin A content	
	µg/gFW	µg/gDW
Control	28.71 ± 3.22^{c}	2.90 ± 0.32^{ab}
50mM	32.42 ± 0.41^{bc}	3.42 ± 0.043^{ab}
100mM	42.48 ± 2.22^{abc}	4.35 ± 0.22^{ab}
150mM	63.45 ± 4.27^{a}	6.40 ± 0.43^{ab}
200mM	51.95 ± 11.69^{ab}	6.05 ± 0.203^{a}
250mM	49.16 ± 6.34^{abc}	5.18 ± 0.94^{ab}

3.12 In-vivo histochemical detection of ROS, cell death, and stem anatomy

Reactive oxygen species (ROS) were visualized with the help of the histochemical staining technique. The DAB and NBT stained the leaves for localization of the accumulation sites of H_2O_2 and $O_2^{\bullet-}$ respectively, in the form of dark patches (Fig. 8a and 8b). The intensities and area of the spots were in accordance with the increasing concentration of the NaCl. *In-vitro* quantification of cell death/membrane damage under the influence of NaCl salt was performed by staining the leaves with Evan's blue dye. Above the 50mM NaCl treatment, salt threatened the membrane integrity of treated leaves as dark blue spots were visualized near the margins of the leaves (Fig. 8c). NaCl strongly affected the anatomical features of the plants as NaCl exposure increased the size of the vasculature, xylogenesis, and area of the pith of the treated plants (Fig. 8d).

3.13 Correlation analysis

The morphological, biochemical, and physiological parameters of salt-treated and non-treated plants were subjected to the correlation analysis (Fig. 9). Many parameters correlated to each other significantly.

We have found a positive correlation between all the morphological and biochemical attributes. Physiological characteristics such as RWC and Fv/Fm were also significantly and positively correlated to each other. On the other hand, defense related parameters like proline, phenol, DPPH, and MDA content negatively correlated to morphological parameters.

4. Discussion

There is only a dearth of knowledge in hand that can justify the exact role of MYB TF, its target genes, mode of action, interaction networks, and binding motifs. Therefore, in the present study identification and characterization of novel MYB protein from *Withania somnifera* was performed and phylogenetic investigation by bootstrap method was accomplished in order to obtain significant hits and evolutionary lineages from other plant species. Topmost hits were found to belong from *Solanum* and *Capsicum* MYB genes. This result was in accordance to the recent findings of Tripathi et al. (2020) in which, they have performed evolutionary relationship of *W. somnifera* AP2/ERF gene with other members of Solanaceae family and obtained top hits from the conserved KYRG domains of *S. lycopersicum*, *C. annum*, *N. tabacum*, *S. tuberosum* etc. Maximum parsimony and UPGMA bootstraping of WsMYB34 with relevant homologue have clustered *W. somnifera* with members of *Capsicum* in close proximity (Mehmood et. al. 2020). This phylogenetic analysis advocated the close evolutionary relationship, monophyletic origin, and recent divergence of WsMYB34 from its wild homologue. On the other hand, MYB family TFs from other Solanaceous members such as species of *Nicotiana* showed paraphyletic relationship with WsMYB34. Likewise, many stress responsive MYB proteins from model plants like rice and Arabidopsis also shared conserved sequence from WsMYB34 protein. Each available TF is categorized and characterized by the specific signature conserved domains. Thus, MSA of WsMYB34 protein was executed that depicted the presence of both functional domains (R2 and R3), at N- terminus of our novel protein as well as in MYB proteins of other members of the Solanaceae family. The strong conservation among amino acid sequences, covering R2 and R3 DNA binding domains from WsMYB34 protein and in its all homologous proteins was observed. This clarifies the critical and indispensable role of MYB TF in adaptation against various stresses. In spite of this, we have found amino acid substitution (replacement of tryptophan by another aromatic amino acid *viz* phenylalanine) inside R3 DNA binding domain. Our results were found in accordance to the report of Ambawat et al. (2013) as they stated the amino acid substitution of first tryptophan residue of R3 domain by phenylalanine, which might have taken place in order to adopt adverse environmental changes. Outcomes of PROSITE and SMART data revealed highly variable nature of C-terminus end of WsMYB34 protein which may play significant role in regulatory activities (Ambawat et al. 2013). The functionality of a protein (TF) can be greatly understood with the help of its 3-D model because these compounds are active in their tertiary form and this form is multiple times more conservative than primary form (Illergård et al. 2009). We modelled our WsMYB34 protein by using available experimentally resolved templates and also checked the reliability of refined predicted model. Authenticity of our model at quantitative parameters (as depicted by VADAR tool) showed it to be more superior and reliable as compared to experimentally resolved templates. Again, qualitative accuracy was also found to be more authenticated for our model, that was further analyzed with the help of various

tools like RAMPAGE, PDBsum server of PROCHECK, MolProbity, ProSA, ERRAT, Verify 3D, QMEAN, and Resprox. In *Withania*, there is no report available, detailing the structural and functional characterization of the MYB protein and its role in combating abiotic stresses. So, our report may provide a significant insight to understand the role of MYB TF in salt tolerance in *W. somnifera* by unravelling the potential active sites, target specific DNA binding capacity, and enhancing secondary metabolism by *in-vitro* and computational approaches. Structural prediction of domain and topological features of modelled protein can be analyzed by performing superimposition of target protein on its experimentally available crystal structures of templates. As depicted by SWISS-MODEL and Superpose software, our modelled protein showed high structural affinity with 6kks, 1h8a, and 3zqc templates as compared to 1a5j. These superimposition results were attested in terms of RMSD values for alpha carbons and backbone atoms of the templates. Further, alignment results from MultiAlin tool also revealed the conserved nature of R2 and R3 domains. Thus, it can be emphasised that the crystal structure of templates along with predicted 3D-model showed more structural similarity rather than sequence similarity thereby attesting to the fact that during the evolutionary period proteins drifted away due to remarkable structural constraints. By bioinformatic approach, gene and attributes of their products can be uniformly described on the basis of all three ontologies i.e. cellular, biological, and molecular functionalities with aid of gene ontology (GO) terms (Rhee et al. 2008). In the present study, CATH server represented the GO terms for WsMYB34 protein which was further analyzed by clustering and scatter plot diagram generated by hypergeometric test distribution of ReviGO. In this context, we found total five GO terms denoting biological processes i.e., for jasmonic acid (GO: 0009753), wounding stress (GO: 0009611), salt stress (GO: 0009651), and UV exposure (GO: 0010224), and regulation of transcription (GO: 0006355) which again confirms the role of MYB TF in combating salt stress. While, four terms were dedicated for molecular functions i.e., protein binding (GO: 0005515), DNA binding (GO: 0043565), sequence specific DNA binding (GO: 0003677), and sequence specific transcription factor activity (GO: 0003700). The results of Cello2GO showed the Subcellular localization of WsMYB34 to reside mainly in nuclear region having score value- 2.44 with 49% probability mostly involved in response to stress, N_2 metabolism, and other biosynthetic processes. In the recent past years, several studies pertaining to gene ontological analysis have been also reported in Medicago and wheat in order to decipher role of this protein in abiotic stress tolerance (Zhou et al. 2019; Wei et al. 2020). There are several research works depicting the combinatorial role of MYB in environmental stress with several TFs like WRKY, WD-40, and bHLH by binding preferentially with major groove of target DNA at C/TAACG/TG (Kim et al. 2012; Choi et al. 2017). This interaction is supported by active involvement of R2 and R3 domains (tryptophan rich alpha helices) in site specific binding on the gene. Based on above findings, our result corroborates with the fact that active SANT domain of MYB protein binds actively with C/TAACG/TG nucleotide sequence of target gene. To attest the role of MYB TF in induced secondary metabolism under NaCl stress in *W. somnifera*, we analyzed *cis*- regulatory DNA element i.e., CAACGG in *CYP85A69* promoter of the same plant and docked it with predicted 3D model of WsMYB34 protein and obtained a good score (9694) with negative ACE value covering 1350.20 area that further attested the reliability of the DNA- protein interaction network. Overall, these findings conclude the synergistic role of MYB TF in combating biotic and abiotic stresses (Kim et al. 2012). Thus, on the basis of *in-silico* findings, we have performed the *in-vitro* techniques to validate these results. The expression

analysis of the genes involved in Withanolide synthetic pathway (MVA; mevalonate pathway and MEP; methylerythritol 4-phosphate pathway genes) was performed along with the transcript encoding putative WsMYB34 transcription factor. Results of semi-quantitative RT-PCR have shown enhanced expressivity of *HMGR, HMGS, DXS, FPPS, DWF1, DXR, SMO1, FK, HYD1*, and *SMT1* genes under the exposure of NaCl (Fig. 7). Similarly, enhanced expression of *WsMYB34* also shows its relationship with the terpene biosynthesis that is also observed previously in *Mentha spicata* for monoterpene and in *Betula platyphylla* against MeJ and SA for triterpenoid (Reddy et al. 2017; Yin et al. 2020). Further, the real time PCR results affirmed the maximum up-regulation of *SMT1, DXR*, and *DWF1*, and *WsMYB34* genes after the exposure of 150mM NaCl treatment. Similarly, flavonoid synthesizing genes were also induced by NaCl stress. NaCl-induced up-regulation in expressivity of withanolide and flavonoid synthetic genes and transcript encoding MYB TF was observed. Up-regulation in the *WsMYB34* gene may be related with its involvement in enhanced trichome organogenesis/development, induction in anthocyanin production, and increased expression of secondary metabolism related genes (Plett et al. 2010; Reddy et al. 2017). The chromatography and spectrophotmetric analysis attested the outcomes of expression data as, NaCl elicitated the secondary metabolites like Withaferin A and flavonoid by many fold. Plants are immotile in nature thus, during the course of evolution and repeatedly changing environment, they have developed complex and mechanistic response networks involving various genes and regulatory transcription factors to adopt it. Due to anthropogenic interference and changes in natural factors, there is a marked dearth of chresard water and surge in soil and water salinity especially from the beginning of 21st century (Munns 2002). Salt causes physiological drought stress in plants thus, it is justified that under saline conditions, plants face double degree of stress i.e., of desiccation as well as of osmotic imbalances caused by ROS toxicity. Further the sodic water limits the growth and yield of plants in accordance to doses of NaCl. In medicinal plants, salt targets both primary and secondary metabolism by altering the gene expression and transcript levels of related TFs and genes. Due to the immense medicinal property of Ashwagandha, elicitation methods have been implemented on this plant by many researchers since past decades to enhance the biosynthesis of pharmacologically active components i.e., Withanolides (Mir et al. 2015; Mishra and Sangwan 2019). In spite of these works, NaCl- mediated metabolic dynamics is not thoroughly studied yet. So, to our knowledge, this is the first report depicting the effect of NaCl on morphology, metabolism and gene expression along with *in-silico* data analysis of MYB TF in *Withania somnifera*. Our findings depicted the negative regulation of NaCl on plant morphology, pigmentation, and photosynthesis. As shown in Table 3, a linear and significant decrease in stem height (14.7-78.87%), FW (20-62.22%), DW (17.77-60%), and leaf morphology was recorded under NaCl stress. These findings were in accordance to the results with *Jatropha curcas* L. seedlings *Zea mays*, *Solanum stoloniferum*, and *S. bulbosum* under different concentrations of NaCl (Gao et al. 2008; Azooz et at. 2009; Daneshmand et al. 2010). This may be due to deploying osmotic stress as a result of elevated sodium ions which drive water away from plant cells and ultimately affect turgor pressure (Rahneshan et al. 2018). The decline in morphological features gave indication towards low water uptake in treated plants, which was further attested by calculating RWC percentage. A gradual decrease in RWC (9.1–24.4%) indicated the weak competency of treated plants to withhold water under the influence of salinity. Salinity is also known to decrease the RWC in a variety of plants like *Artemisia annua* and *Pistacia vera* L., *Polygonum*

equisetiforme, etc (Rahneshan et al. 2018; Boughalleb et al. 2020). Next, our study delineated a significant and linear decline in the activity of the photosynthetic apparatus of treated plants with respect to the control plants (Table 4). This result suggests degradation and /or suppression in chlorophyll synthesis, or oxidation of pigments as well as stomatal closure as an adaptive measure to check water loss under salinity (Wang et al. 2019). Carotenoid content of treated plants were also found to decline significantly. This finding was in consistence with the previous report of Taïbi et al. (2016), performed on *Phaseolus vulgaris*. Besides providing colour, anthocyanins also provide defence to the plants, especially under stress, which was estimated to enhance upto 150mM NaCl and slight decrease was observed after 200 and 250mM concentration. Although the increase was insignificant as compared to control sets but according to Kaliamoortiiy and Rao (1994), this upsurge is may be due to the accumulation of the pigment under salinity stress. Photosynthetic efficiency of PSII system of light reaction is estimated by chlorophyll fluorescence (Fv/Fm). According to Akhter et al. (2021), this ratio can be used as most feasible explanation for the physiological health of plants. In the present work, a significant decline in the chlorophyll fluorescence was obtained in treated sets of plants. This notion suggests that NaCl mediated ROS stress inhibited photosynthetic apparatus by damage of the antenna complex i.e., D1 protein of PSII reaction centre (Ahmed et al., 2002). Proline acts as stress marker in the plants and is widely known to be involved in mechanism orchestrated for defence strategies. Under the influence of ROS stress, proline acts as both free radical scavenger as well as a membrane stabilizer. Since, proline work as a protective entity (osmolyte), we have found significant enhancement in its content, in a dose-dependent manner (Table 4). This result is in accordance with the previous works, performed on *Polygonum equisetiforme* (Boughalleb et al. 2020). Phenols and polyphenols are the largest group of metabolites that provide protection against various stresses (Šamec et al. 2021). We observed significant and dose-dependent increment in the total phenolics of the NaCl- treated plants in comparison to non-treated control plants which are in obedience to the result of Baâtour et al. (2013). Some other osmolytes like soluble sugar and free proteins also provide osmoprotection to the plants in various stress conditions (Jogawat 2019). We observed a significant increase in the protein content upto 150mM NaCl which get decline after 200mM NaCl. Similar trend was also recorded in *Broussonetia papyrifera* by Zhang et al. (2013). Accumulation of protein under salinity stress may provide a base for the synthesis and modification of damaged cell wall. Further, we estimated the malondialdehyde (MDA) content in order to estimate lipid peroxidation and found NaCl-induced increment in membrane damage and/or leakage in treated plants. Same pattern of enhanced membrane leakage has also been reported in *Polygonum equisetiforme* (Boughalleb et al. 2020). After the uptake of NaCl generated ions, plenty of ROS generation have been observed in the plant cells which can be mitigated by free radical scavenging mechanisms. In this regard, accumulation of excess ROS in the form of $O_2^{\bullet-}$ and H_2O_2 was investigated by staining with NBT and DAB respectively. Figures 8 and 8b showed elevated accumulation of ROS according to increasing dose of NaCl. Further, for NaCl induced antioxidative capacity, DPPH (free radical scavenging activity) assay was performed. The dose dependent increment in % inhibition of free radicals upto 200mM NaCl concentration was observed. Our results were corroborated by the finding of Yan et al. (2017) and Boughalleb et al. (2020) as they observed enhanced DPPH activity NaCl treated *Lonicera japonica* and *Polygonum* respectively. Further, effect of NaCl on stem anatomical features and on trichome density was also observed. As

depicted in Fig. 8d salt treatment caused dose dependent increase in the cuticle thickness, vascular bundle, and pith. According to Dolatabadian et al. (2011), this may be due to deposition of cutin layer on the surface of stem in order to protect the plant against osmotic stresses. Our observations are in consistent with the results of Atabayeva et al. (2013), in which they treated barley seedlings with NaCl. The trichomes were also observed on the surface of plants. Because in many medicinal plants, glandular trichomes are known to be repository of bioactive secondary metabolites, in the case of *W. somnifera* our knowledge is limited to know exact site of deposition of withanolides. Moreover, researchers have hypothesized that in this plant, withanolides are accumulated in secretary glandular trichomes (Munien, 2015). In this study, we visualized increment in number of leaf surface trichomes after the exposure to salinity stress, similar to salinity induced increase in trichome density in *Mentha pulegium* L. and *Schizonepeta tenuifolia* (Karray-Bouraoui et al. 2009; Zhou et al. 2018). The Withaferins from this plant is reported to play important role in defence mechanism against abiotic stresses along with various regulatory transcription factors (Meraj et al. 2020). In our study, chromatographic results have depicted significant increase in the withaferin A content upto 150mM NaCl treatment. NaCl induced induction in the synthesis of secondary metabolites has already reported in many plants like safflower and *Spinacia oleracea* L. (Gengmao et al. 2015; Muchate et al. 2019). At last, on the basis of *in-silico* analysis and experimental outcomes, we have constructed a possible hypothetical diagram to demonstrate the effect of salt on growth and metabolism in *W. somnifera* and orchestration of withanolide genes under the influence of WsMYB34 protein (Fig. 10). This model linked the plants primary and secondary metabolism and depicted the induction of various biochemical properties (such as proline, phenol, protein, and anthocyanin) and secondary metabolites in *W. somnifera* by ROS, generated by NaCl. From model it is clearly visible that ROS burst results in membrane damage and cell death which further results in free radical scavenging activity. In spite of this, molecular studies also validated our findings as salt mediated the up-regulation in withanolide synthesizing and *WsMYB34* gene. The *WsMYB34* gene was also found to bind to the promoter region of *CYP85A69* gene which is responsible for terpene accumulation. Thus, on the basis of all findings it may be concluded that optimum level of NaCl reduces the growth and induces plant secondary metabolism via up-regulating secondary metabolic pathway genes, involving WsMYB34 as regulator.

5. Conclusion

The pattern of secondary metabolite genes and *WsMYB34* gene expression revealed the involvement of MYB34 TF in salt tolerance in *Withania somnifera*. The *in-silico* based microarray analysis also revealed the role of MYB proteins in combating abiotic stresses. Further, *in-silico* structural and functional characterization of WsMYB34 protein revealed the highly conserved nature of the N-terminus of WsMYB34 protein showing 8–10 times more conserved nature than the amino acid sequences demonstrating active participation of MYB TF amongst plants in environmental stress tolerance. Moving deeper in this direction, some more computational approaches have delivered crucial data regarding sequence conservation, motifs, active domains, phylogenetic origin, and functional interactomes. In the present study, possible mechanism of MYB TF in regulation of secondary metabolism is also analyzed.

The presence of CAACTG regulatory DNA sequence (which is target for MYB protein) in the *CYP85A69* gene of *W. somnifera* further confirms its involvement in withanolides synthesis as, the TF binding may up-regulate the withanolide production. Due to dearth of proper knowledge regarding possible function of MYB TFs in mitigation of abiotic stress tolerance in *W. somnifera*, this study will surely provide the base to unravel the mechanistic approaches and synergistic networks of MYB proteins in enhancement of defence related strategies and improved secondary metabolism under adverse environmental conditions.

Declarations

6. Conflict of interest

There is no any conflict of interest between authors.

7. Author's contributions

LS and SPR designed the experimental works. LS performed experimentation and wrote the whole manuscript. BM helped in biochemical analysis. SP helped in phylogenetic assessment and microarray analysis. KKR contributed in assessment of molecular data. SPR supervised the whole work and designed the final manuscript by providing critical feedback.

8. Acknowledgements

We are thankful to CAS- Botany (BHU) and DST-FIST for providing fund and other facilities to Department of Botany, Institute of Science, Banaras Hindu University. We also show gratitude towards Central Instrumental Facility (CIL), Department of Botany, BHU for providing HPLC and Spectrophotometer. All the authors are thankful to Interdisciplinary School of Life-Sciences (ISLS) – Banaras Hindu University from where we got facility in the form of fluorescent microscopy. Lakee Sharma is greatly thankful to CSIR-New Delhi for providing financial support.

References

1. Ahmed S, Nawata E, Hosokawa M, Domae Y, Sakuratani T (2002) Alterations in photosynthesis and some antioxidant enzymatic activities of mungbean subjected to waterlogging. Plant Sci 163:117–123
2. Akhter MS, Noreen S, Mahmood S, Ashraf M, Alsahli AA, Ahmad P (2021) Influence of salinity stress on PSII in barley (Hordeum vulgare L.) genotypes, probed by chlorophyll-a fluorescence. J King Saud Univ Sci 33:101239
3. Alves MS, Dadalto SP, Gonçalves AB, De Souza GB, Barros VA, Fietto LG (2014) Transcription factor functional protein-protein interactions in plant defense responses. Proteomes 2:85–106
4. Amarr V, Nori P, Zhu H (2017) Spearmint R2R3â MYB transcription factor MsMYB negatively regulates monoterpene production and suppresses the expression of geranyl diphosphate synthase large subunit (MsGPPS. LSU). Plant Biotechnol J

5. Ambawat S, Sharma P, Yadav NR, Yadav RC (2013) MYB transcription factor genes as regulators for plant responses: an overview. Physiol Mol Biol Pla 19:307–321
6. Atabayeva S, Nurmahanova A, Minocha S, Ahmetova A, Kenzhebayeva S, Aidosova S, Nurzhanova A, Zhardamalieva A, Asr S, Alybayeva R (2013) The effect of salinity on growth and anatomical attributes of barley seedling (Hordeum vulgare L.). Afr J Biotechnol 12:2366–2377
7. Azooz M, Ismail A, Elhamd MA (2009) Growth, lipid peroxidation and antioxidant enzyme activities as a selection criterion for the salt tolerance of maize cultivars grown under salinity stress. Int J Agric Biol 11:21–26
8. Baâtour O, Mahmoudi H, Tarchoun I, Nasri N, Trabelsi N, Kaddour R, Zaghdoudi M, Hamdawi G, Ksouri R, Lachaâl M (2013) Salt effect on phenolics and antioxidant activities of Tunisian and Canadian sweet marjoram (Origanum majorana L.) shoots. J Sci Food Agr 93:134–141
9. Bailey TL, Williams N, Misleh C, Li WW (2006) MEME: discovering and analyzing DNA and protein sequence motifs. Nucleic Acids Res 34:W369–W373
10. Bates LS, Waldren RP, Teare I (1973) Rapid determination of free proline for water-stress studies. Plant soil 39:205–207
11. Boughalleb F, Abdellaoui R, Mahmoudi M, Bakhshandeh E (2020) Changes in phenolic profile, soluble sugar, proline, and antioxidant enzyme activities of Polygonum equisetiforme in response to salinity. Turk J Bot 44:25–35
12. Butt HI, Yang Z, Gong Q, Chen E, Wang X, Zhao G, Ge X, Zhang X, Li F (2017) GaMYB85, an R2R3 MYB gene, in transgenic Arabidopsis plays an important role in drought tolerance. BMC Plant Biol 17:1–17
13. Castrignano T, De Meo PDO, Cozzetto D, Talamo IG, Tramontano A (2006) The PMDB protein model database. Nucleic Acids Res 34:D306–D309
14. Chang CC, Yang MH, Wen HM, Chern JC (2002) Estimation of total flavonoid content in propolis by two complementary colorimetric methods.J Food Drug Anal10(3)
15. Choi J, Abbai R, Kim Y, Silva J, Rahimi S, Myagmarjav D, Chung I, Kwon W, Yang D (2017) Molecular characterization of MYB transcription factor genes from Panax ginseng. Russ J Plant Physl–– 64:398–409
16. Colovos C, Yeates TO (1993) Verification of protein structures: patterns of nonbonded atomic interactions. Protein Sci 2:1511–1519
17. Daneshmand F, Arvin MJ, Kalantari KM (2010) Physiological responses to NaCl stress in three wild species of potato in vitro. Acta Physiol Plant 32:91–101
18. Das S, Orengo CA (2016) Protein function annotation using protein domain family resources. Methods 93:24–34
19. Dolatabadian A, SANAVY SAMM, Ghanati F (2011) Effect of salinity on growth, xylem structure and anatomical characteristics of soybean. Not Sci Biol 3:41–45

20. Frahry G, Schopfer P (1998) Hydrogen peroxide production by roots and its stimulation by exogenous NADH. Physiol Plant 103:395–404
21. Gao S, Ouyang C, Wang S, Xu Y, Tang L, Chen F (2008) Effects of salt stress on growth, antioxidant enzyme and phenylalanine ammonia-lyase activities in Jatropha curcas L. seedlings. Plant Soil Environ 54:374–381
22. Gengmao Z, Yu H, Xing S, Shihui L, Quanmei S, Changhai W (2015) Salinity stress increases secondary metabolites and enzyme activity in safflower. Ind Crop Prod 64:175–181
23. González L, González-Vilar M (2001) Determination of relative water content. Handbook of plant ecophysiology techniques. Springer, pp 207–212
24. Greenway H, Munns R (1980) Mechanisms of salt tolerance in nonhalophytes. Ann Rev Plant Physio 31:149–190
25. Heath RL, Packer L (1968) Photoperoxidation in isolated chloroplasts: I. Kinetics and stoichiometry of fatty acid peroxidation. Arch Biochem Biophys 125:189–198
26. Hoagland DR, Arnon DI (1950) The water-culture method for growing plants without soil. Circular. California agricultural experiment station. 1950;347(2nd edit)
27. Illergård K, Ardell DH, Elofsson A (2009) Structure is three to ten times more conserved than sequence—a study of structural response in protein cores. Proteins Struct Funct Bioinform 77:499–508
28. Imeh U, Khokhar S (2002) Distribution of conjugated and free phenols in fruits: antioxidant activity and cultivar variations. J Agr Food Chem 50:6301–6306
29. Apoorva JD, Pandey-Rai S, Agrawal SB (2021) Untangling the UV-B radiation-induced transcriptional network regulating plant morphogenesis and secondary metabolite production. Environ Exp Bot 192:104655
30. Jin H, Martin C (1999) Multifunctionality and diversity within the plant MYB-gene family. Plant Mol Biol 41:577–585
31. Jogawat A (2019) Osmolytes and their role in abiotic stress tolerance in plants. Molecular plant abiotic stress: biology and biotechnology 91–104
32. Kaliamoortiiy S, Rao A (1994) Effect of salinity on anthocyanin accumulation in the root of maize. Science 248:1637–1638
33. Karray-Bouraoui N, Rabhi M, Neffati M, Baldan B, Ranieri A, Marzouk B, Lachaâl M, Smaoui A (2009) Salt effect on yield and composition of shoot essential oil and trichome morphology and density on leaves of Mentha pulegium. Ind Crop Prod 30:338–343
34. Kim JH, Kim BG, Ahn JH (2012) Determination of the MYB Motif Interacting with WD40 and Basic Helix Loop Helix Proteins. J Appl Biol Chem 55:67–70
35. Larkin MA, Blackshields G, Brown NP, Chenna R, McGettigan PA, McWilliam H, Valentin F, Wallace IM, Wilm A, Lopez R (2007) Clustal W and Clustal X version 2.0. Bioinformatics 23:2947–2948
36. Laskowski RA (2009) PDBsum new things. Nucleic Acids Res 37:D355–D359

37. Lowry O, Rosebrough N, Farr AL, Randall R (1951) Protein measurement with the Folin phenol reagent. J Biol Chem 1(1):265–275
38. Maiti R, Van Domselaar GH, Zhang H, Wishart DS (2004) SuperPose: a simple server for sophisticated structural superposition. Nucleic Acids Res 32:W590–W594
39. Mancinelli A, Yang C-PH, Lindquist P, Anderson O, Rabino I (1975) Photocontrol of anthocyanin synthesis: III. The action of streptomycin on the synthesis of chlorophyll and anthocyanin. Plant Physiol 55:251–257
40. Maurya B, Rai KK, Pandey N, Sharma L, Goswami NK, Rai SP (2019) Influence of salicylic acid elicitation on secondary metabolites and biomass production in in-vitro cultured Withania coagulans (L.) Dunal. Plant Arch 19:1045–1308
41. Mehmood F, Ubaid Z, Bao Y, Poczai P, Mirza B (2020) Comparative plastomics of Ashwagandha (Withania, Solanaceae) and identification of mutational hotspots for barcoding medicinal plants. Plants 9:752
42. Meraj TA, Fu J, Raza MA, Zhu C, Shen Q, Xu D, Wang Q (2020) Transcriptional factors regulate plant stress responses through mediating secondary metabolism. Genes 11:346
43. Mir BA, Mir SA, Khazir J, Tonfack LB, Cowan DA, Vyas D, Koul S (2015) Cold stress affects antioxidative response and accumulation of medicinally important withanolides in Withania somnifera (L.) Dunal. Ind Crop Prod 74:1008–1016
44. Mishra B, Singh Sangwan N (2019) Amelioration of cadmium stress in Withania somnifera by ROS management: active participation of primary and secondary metabolism. Plant Growth Regul 87:403–412
45. Mocready R, Guggolz J, Silviera V, Owens H (1950) Determination of starch and amylose in vegetables. Application to peas. Anal Chem 22:1156–1158
46. Mohamed BB, Aftab B, Sarwar MB, Rashid B, Ahmad Z, Hassan S, Husnain T (2017) Identification and Characterization of the Diverse Stress-Responsive R2R3-RMYB Transcription Factor from Hibiscus sabdariffa L. Int J Genomics 2017
47. Muchate NS, Rajurkar NS, Suprasanna P, Nikam TD (2019) NaCl induced salt adaptive changes and enhanced accumulation of 20-hydroxyecdysone in the in vitro shoot cultures of Spinacia oleracea (L.). Sci Rep 9:1–10
48. Munien P, Naidoo Y, Naidoo G (2015) Micromorphology, histochemistry and ultrastructure of the foliar trichomes of Withania somnifera (L.) Dunal (Solanaceae). Planta 242:1107–1122
49. Munns R (2002) Comparative physiology of salt and water stress. Plant Cell Environ 25:239–250
50. Munns R, Tester M (2008) Mechanisms of salinity tolerance. Annu Rev Plant Biol 59:651–681
51. Nakashima K, Takasaki H, Mizoi J, Shinozaki K, Yamaguchi-Shinozaki K (2012) NAC transcription factors in plant abiotic stress responses. BBA-Gene Regul Mech 1819:97–103
52. Parida AK, Das AB (2005) Salt tolerance and salinity effects on plants: a review. Ecotox Environ Safe 60:324–349

53. Plett JM, Wilkins O, Campbell MM, Ralph SG, Regan S (2010) Endogenous overexpression of Populus MYB186 increases trichome density, improves insect pest resistance, and impacts plant growth. Plant J 64:419–432
54. Porra R, Thompson W, Kriedemann P (1989) Determination of accurate extinction coefficients and simultaneous equations for assaying chlorophylls a and b extracted with four different solvents: verification of the concentration of chlorophyll standards by atomic absorption spectroscopy. BBA-Bioenergetics 975:384–394
55. Rahneshan Z, Nasibi F, Moghadam AA (2018) Effects of salinity stress on some growth, physiological, biochemical parameters and nutrients in two pistachio (Pistacia vera L.) rootstocks. J Plant Interact 13:73–82
56. Rai KK, Rai N, Rai SP (2019) Prediction and validation of DREB transcription factors for salt tolerance in Solanum lycopersicum L.: An integrated experimental and computational approach. Environ Exp Bot 165:1–18
57. Reddy VA, Wang Q, Dhar N, Kumar N, Venkatesh PN, Rajan C, Panicker D, Sridhar V, Mao HZ, Sarojam R (2017) Spearmint R2R3-MYB transcription factor Ms MYB negatively regulates monoterpene production and suppresses the expression of geranyl diphosphate synthase large subunit (Ms GPPS. LSU). Plant Biotechnol J 15:1105–1119
58. Roy A, Yang J, Zhang Y (2012) COFACTOR: an accurate comparative algorithm for structure-based protein function annotation. Nucleic Acids Res 40:W471–W477
59. Sabir F, Sangwan RS, Kumar R, Sangwan NS (2012) Salt stress-induced responses in growth and metabolism in callus cultures and differentiating in vitro shoots of Indian ginseng (Withania somnifera Dunal). J Plant Growth Regul 31:537–548
60. Šamec D, Karalija E, Šola I, Vujčić Bok V, Salopek-Sondi B (2021) The role of polyphenols in abiotic stress response: The influence of molecular structure. Plants 10:118
61. Schneidman-Duhovny D, Inbar Y, Nussinov R, Wolfson HJ (2005) PatchDock and SymmDock: servers for rigid and symmetric docking. Nucleic Acids Res 33:W363–W367
62. Sharma A, Rather GA, Misra P, Dhar MK, Lattoo SK (2019) Jasmonate responsive transcription factor WsMYC2 regulates the biosynthesis of triterpenoid withanolides and phytosterol via key pathway genes in Withania somnifera (L.) Dunal. Plant Mol Biol 100:543–560
63. Sharma V (2013) HPLC-PDA method for quantification of Withaferin-A and Withanolide-A in diploid (n = 12) and tetraploid (n = 24) cytotypes of “Indian Ginseng” Withania somanifera (L.) Dunal from North India. Int J Indig Med Plants 46:1245–1250
64. Singh AK, Kumar SR, Dwivedi V, Rai A, Pal S, Shasany AK, Nagegowda DA (2017) A WRKY transcription factor from Withania somnifera regulates triterpenoid withanolide accumulation and biotic stress tolerance through modulation of phytosterol and defense pathways. New Phytol 215:1115–1131
65. Singh KB, Foley RC, Oñate-Sánchez L (2002) Transcription factors in plant defense and stress responses. Curr Opin Plant Biol 5:430–436

66. Supek F, Bošnjak M, Škunca N, Šmuc T (2011) REVIGO summarizes and visualizes long lists of gene ontology terms. PLoS ONE 6:e21800
67. Taïbi K, Taïbi F, Abderrahim LA, Ennajah A, Belkhodja M, Mulet JM (2016) Effect of salt stress on growth, chlorophyll content, lipid peroxidation and antioxidant defence systems in Phaseolus vulgaris L. S Afr J Bot 105:306–312
68. Tak H, Negi S, Ganapathi T (2017) Overexpression of MusaMYB31, a R2R3 type MYB transcription factor gene indicate its role as a negative regulator of lignin biosynthesis in banana. PLoS ONE 12:e0172695
69. Tamura K, Stecher G, Peterson D, Filipski A, Kumar S (2013) MEGA6: molecular evolutionary genetics analysis version 6.0. Mol Biol Evol 30:2725–2729
70. Tang Y, Bao X, Zhi Y, Wu Q, Guo Y, Yin X, Zeng L, Li J, Zhang J, He W (2019) Overexpression of a MYB family gene, OsMYB6, increases drought and salinity stress tolerance in transgenic rice. Front Plant Sci 10:168
71. Thordal-Christensen H, Zhang Z, Wei Y, Collinge DB (1997) Subcellular localization of H2O2 in plants. H2O2 accumulation in papillae and hypersensitive response during the barley—powdery mildew interaction. Plant J 11:1187–1194
72. Tripathi D, Rai KK, Pandey-Rai S (2021) Impact of green synthesized WcAgNPs on in-vitro plant regeneration and withanolides production by inducing key biosynthetic genes in Withania coagulans. Plant Cell Rep 40:283–299
73. Tripathi S, Srivastava Y, Sangwan RS, Sangwan NS (2020) In silico mining and functional analysis of AP2/ERF gene in Withania somnifera. Sci Rep-UK 10:1–12
74. Ullah A, Ul Qamar MT, Nisar M, Hazrat A, Rahim G, Khan AH, Hayat K, Ahmed S, Ali W, Yang X (2020) Characterization of a novel cotton MYB gene, GhMYB108-like responsive to abiotic stresses. Mol Biol Rep 47:1573–1581
75. Wang YH, Zhang G, Chen Y, Gao J, Sun YR, Sun MF, Chen JP (2019) Exogenous application of gibberellic acid and ascorbic acid improved tolerance of okra seedlings to NaCl stress. Acta Physiol Plant 41:1–10
76. Waterhouse A, Bertoni M, Bienert S, Studer G, Tauriello G, Gumienny R, Heer FT, de Beer TAP, Rempfer C, Bordoli L (2018) SWISS-MODEL: homology modelling of protein structures and complexes. Nucleic Acids Res 46:W296–W303
77. Wei Q, Chen R, Wei X, Liu Y, Zhao S, Yin X, Xie T (2020) Genome-wide identification of R2R3-MYB family in wheat and functional characteristics of the abiotic stress responsive gene TaMYB344. BMC Genomics 21:1–16
78. Wiederstein M, Sippl MJ (2007) ProSA-web: interactive web service for the recognition of errors in three-dimensional structures of proteins. Nucleic Acids Res 35:W407–W410
79. Willard L, Ranjan A, Zhang H, Monzavi H, Boyko RF, Sykes BD, Wishart DS (2003) VADAR: a web server for quantitative evaluation of protein structure quality. Nucleic Acids Res 31:3316–3319

80. Xu D, Zhang Y (2011) Improving the physical realism and structural accuracy of protein models by a two-step atomic-level energy minimization. Biophys J 101:2525–2534
81. Xu ZS, Feng K, Que F, Wang F, Xiong AS (2017) A MYB transcription factor, DcMYB6, is involved in regulating anthocyanin biosynthesis in purple carrot taproots. Sci Rep-UK 7:1–9
82. Yan K, Zhao S, Bian L, Chen X (2017) Saline stress enhanced accumulation of leaf phenolics in honeysuckle (Lonicera japonica Thunb.) without induction of oxidative stress. Plant Physiol Bioch 112:326–334
83. Yin J, Sun L, Li Y, Xiao J, Wang S, Yang J, Qu Z, Zhan Y (2020) Functional identification of BpMYB21 and BpMYB61 transcription factors responding to MeJA and SA in birch triterpenoid synthesis. BMC Plant Biol 20:1–22
84. Yon Rhee S, Wood V, Dolinski K, Draghici S (2008) Use and misuse of the gene ontology annotations. Nat Rev Genet 9:509–515
85. Yu CS, Cheng CW, Su WC, Chang KC, Huang S-W, Hwang J-K, Lu C-H (2014) CELLO2GO: a web server for protein subCELlular LOcalization prediction with functional gene ontology annotation. PLoS ONE 9:e99368
86. Zhang M, Fang Y, Ji Y, Jiang Z, Wang L (2013) Effects of salt stress on ion content, antioxidant enzymes and protein profile in different tissues of Broussonetia papyrifera. S Afr J Bot 85:1–9
87. Zhou Q, Jia C, Ma W, Cui Y, Jin X, Luo D, Min X, Liu Z (2019) MYB transcription factors in alfalfa (Medicago sativa): genome-wide identification and expression analysis under abiotic stresses. PeerJ 7:e7714
88. Zhou Y, Tang N, Huang L, Zhao Y, Tang X, Wang K (2018) Effects of Salt Stress on Plant Growth, Antioxidant Capacity, Glandular Trichome Density, and Volatile Exudates of Schizonepeta tenuifolia Briq. Int J Mol Sci 19:252
89. Zhu J (2002) Salt and Drought Stress Signal Transduction in Plants. Annu Rev Plant Biol 53:247–273

Figures

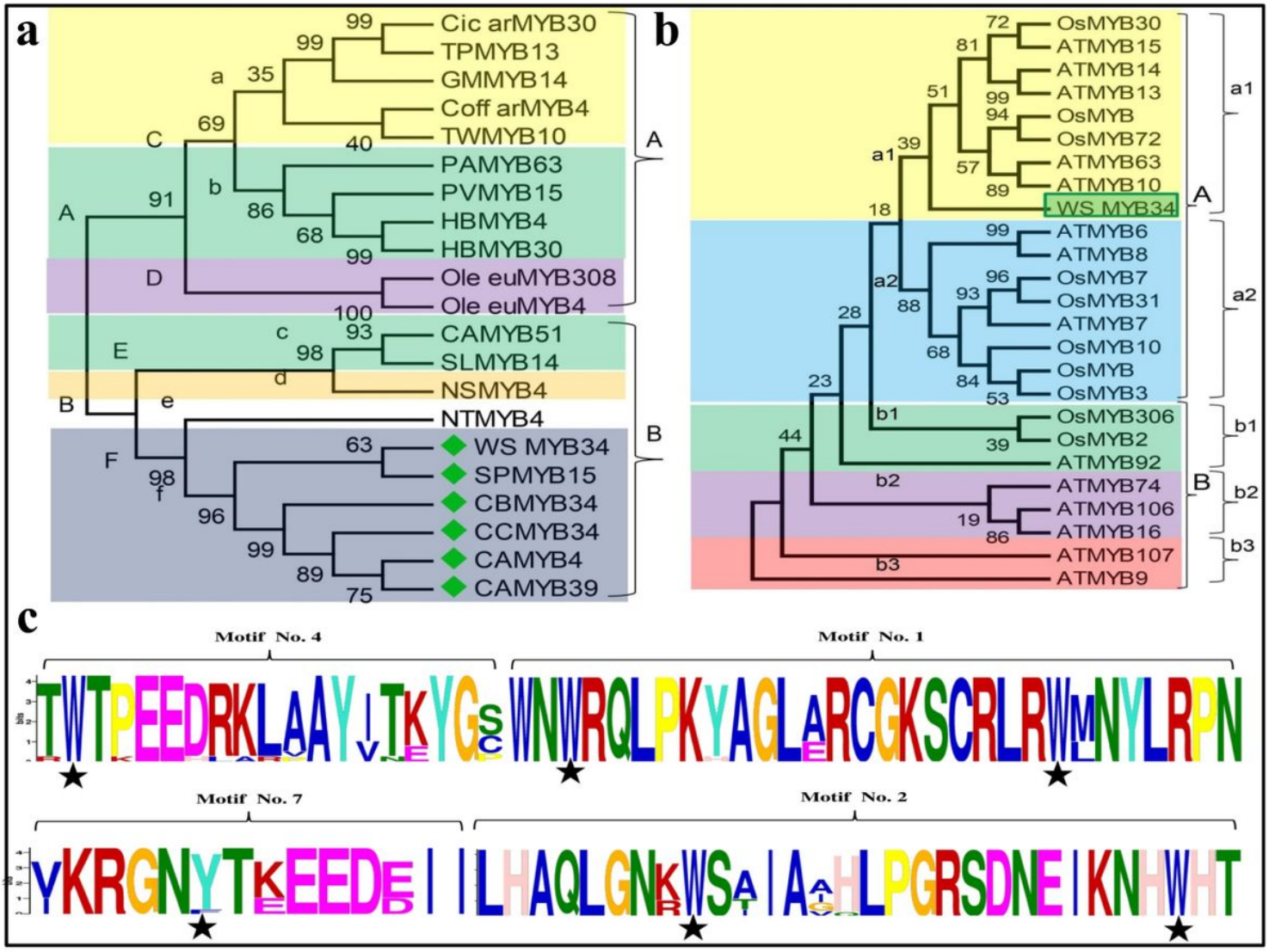


Figure 1

Phylogenetic tree and conserved motifs of WsMYB34 protein sequence. (a) Phylogenetic tree of WsMYB34 protein among all homologues; (b) with other homologues from dicot and monocot model plants rice and Arabidopsis constructed by N-J method of MEGA version 4.0.02; and (c) Conserved motif sequences in the deduced amino acid sequences of WsMYB34 from *W. somnifera* and among homologues of other plants (astrid

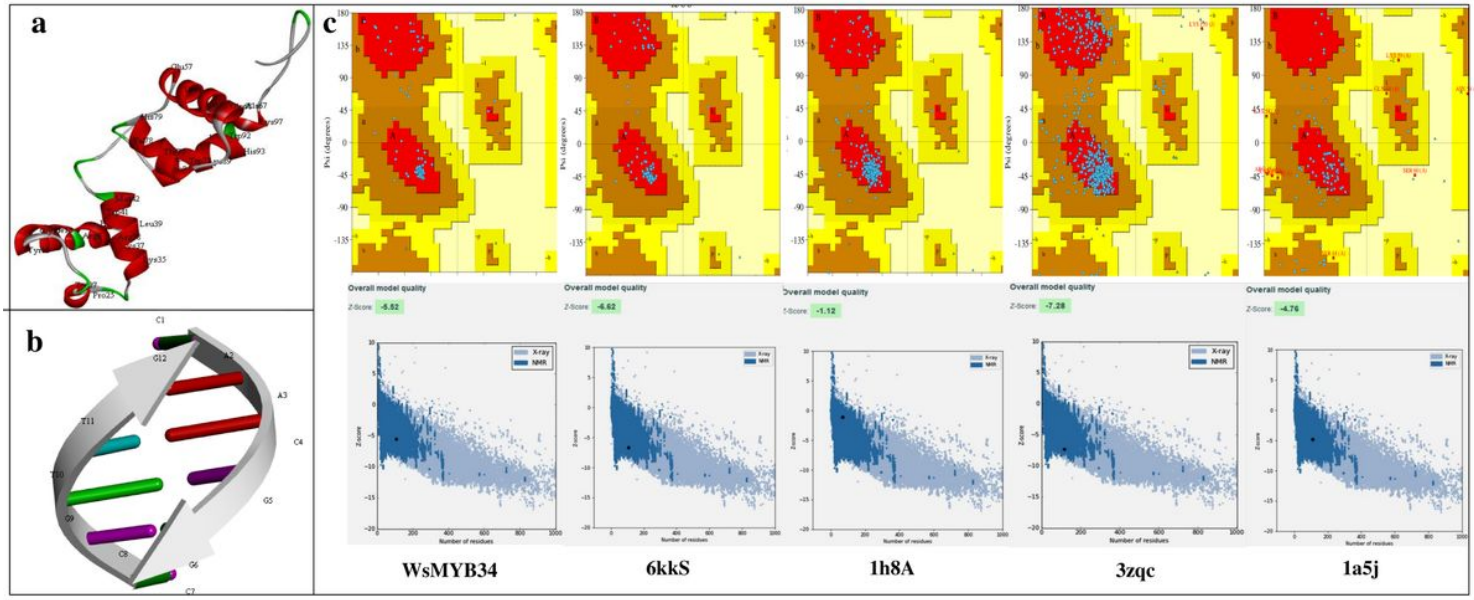
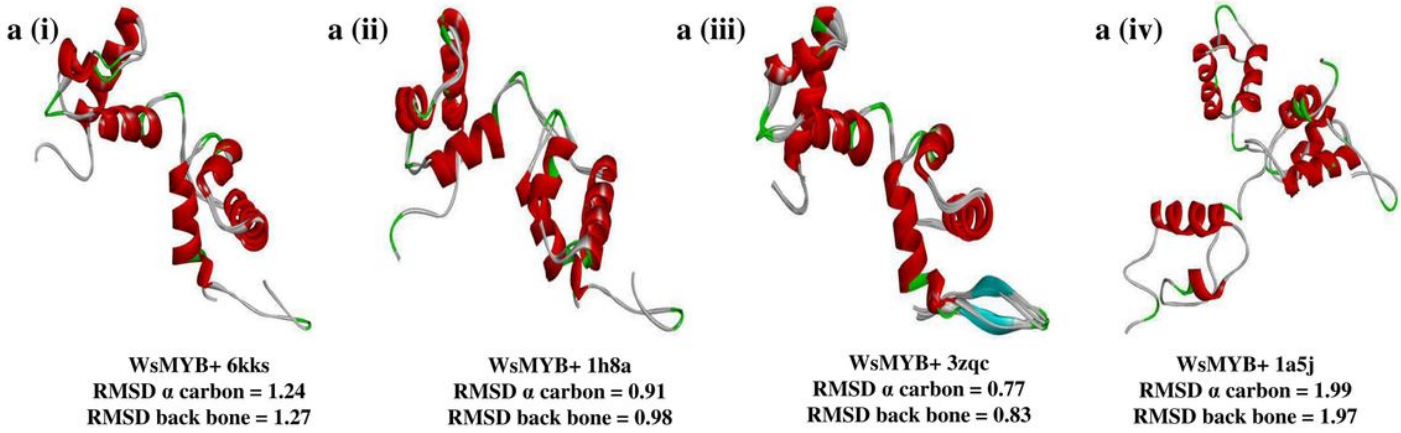


Figure 2

Predicted structures of (a) refined 3-D model of R2 and R3 functional domains of WsMYB34; (b) structure of MYB binding DNA element C/TAACG/TG on promoter of *CYP85A69* gene; and (c) Validation of predicted refined model by qualitative analysis with PROCHECK (Ramachandran plot analysis) and ProSA server (to calculate Z-score)



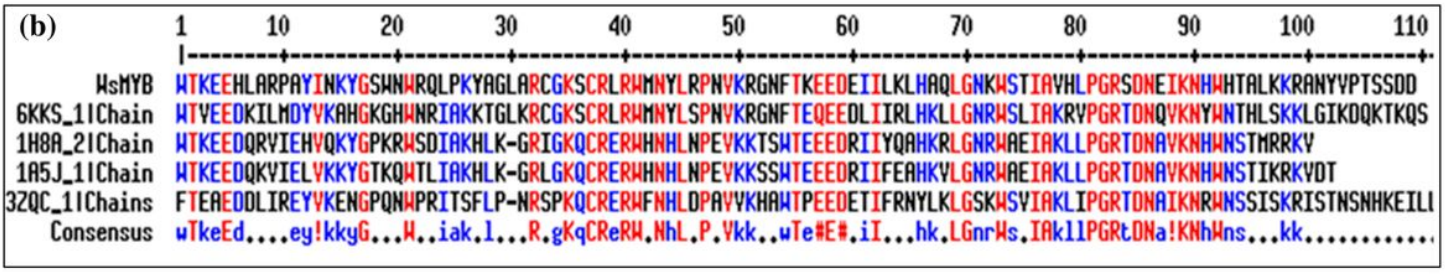
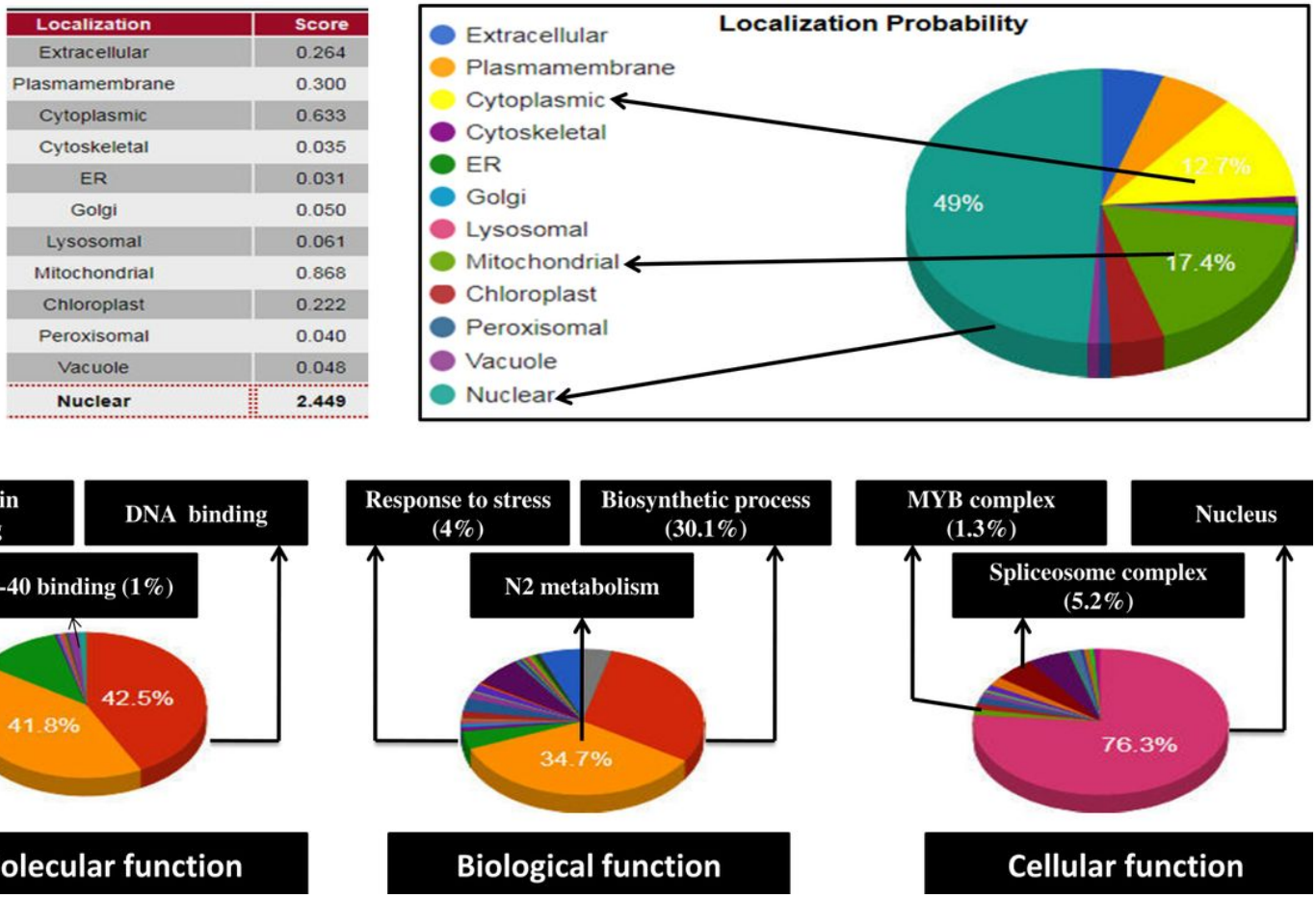


Figure 3

Superimposition analysis (a) between target WsMYB34 protein domain and experimentally resolved templates [a (i)-a (iv)], and (b) sequence conservation between target and template protein and analysis of synonymous and non-synonymous sequence substitution



Localization	Score
Extracellular	0.264
Plasmamembrane	0.300
Cytoplasmic	0.633
Cytoskeletal	0.035
ER	0.031
Golgi	0.050
Lysosomal	0.061
Mitochondrial	0.868
Chloroplast	0.222
Peroxisomal	0.040
Vacuole	0.048
Nuclear	**2.449**

Figure 4

Analysis of functional gene annotation and subcellular localization of WsMYB34 protein by CELLO2GO web server

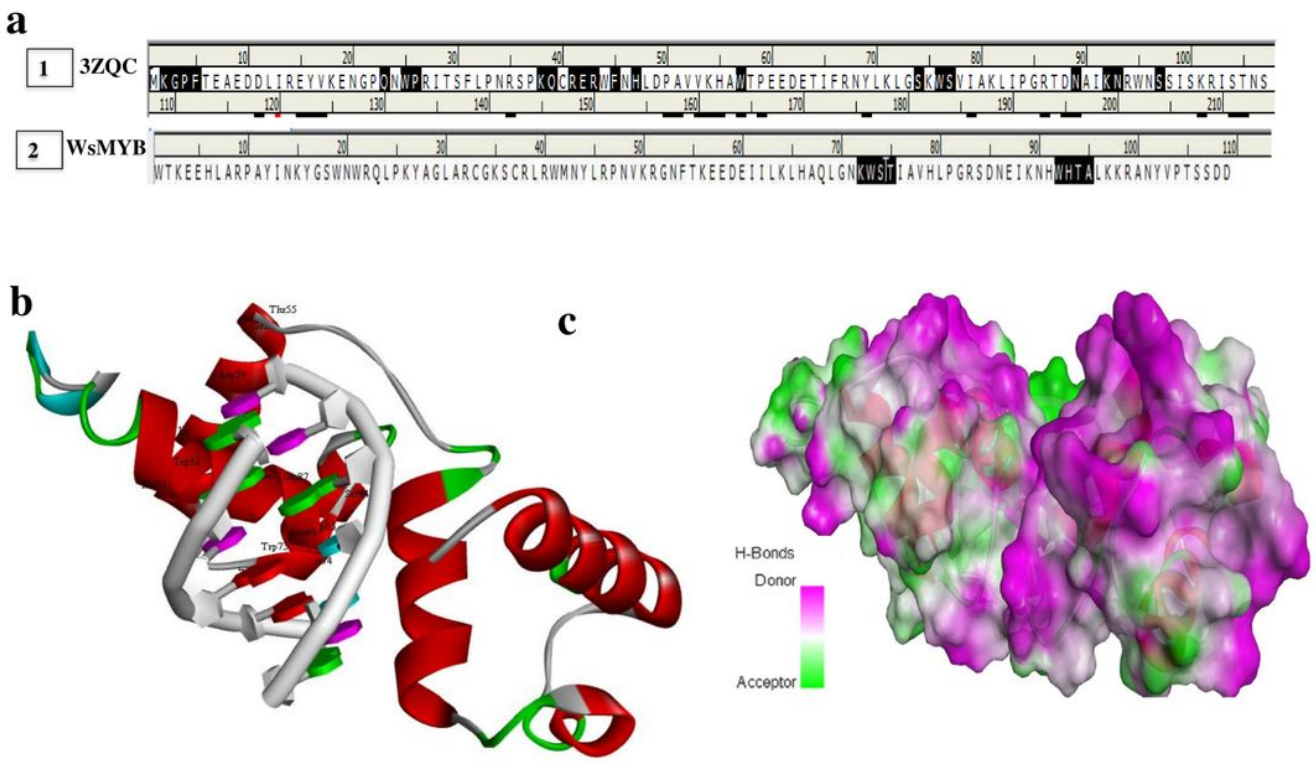


Figure 5

Binding analysis of WsMYB34 protein to promoter of *CYP85A69* gene. (a) A comparative analysis of docked complex with functional motif of WsMYB34 protein and experimentally resolved template 3ZQC, (b) docked complex between WsMYB34 and DNA binding element C/TAACG/TG, and (c) three dimensional topological view of WsMYB34- C/TAACG/TG complex depicting the hydrogen donors and acceptors in the complex

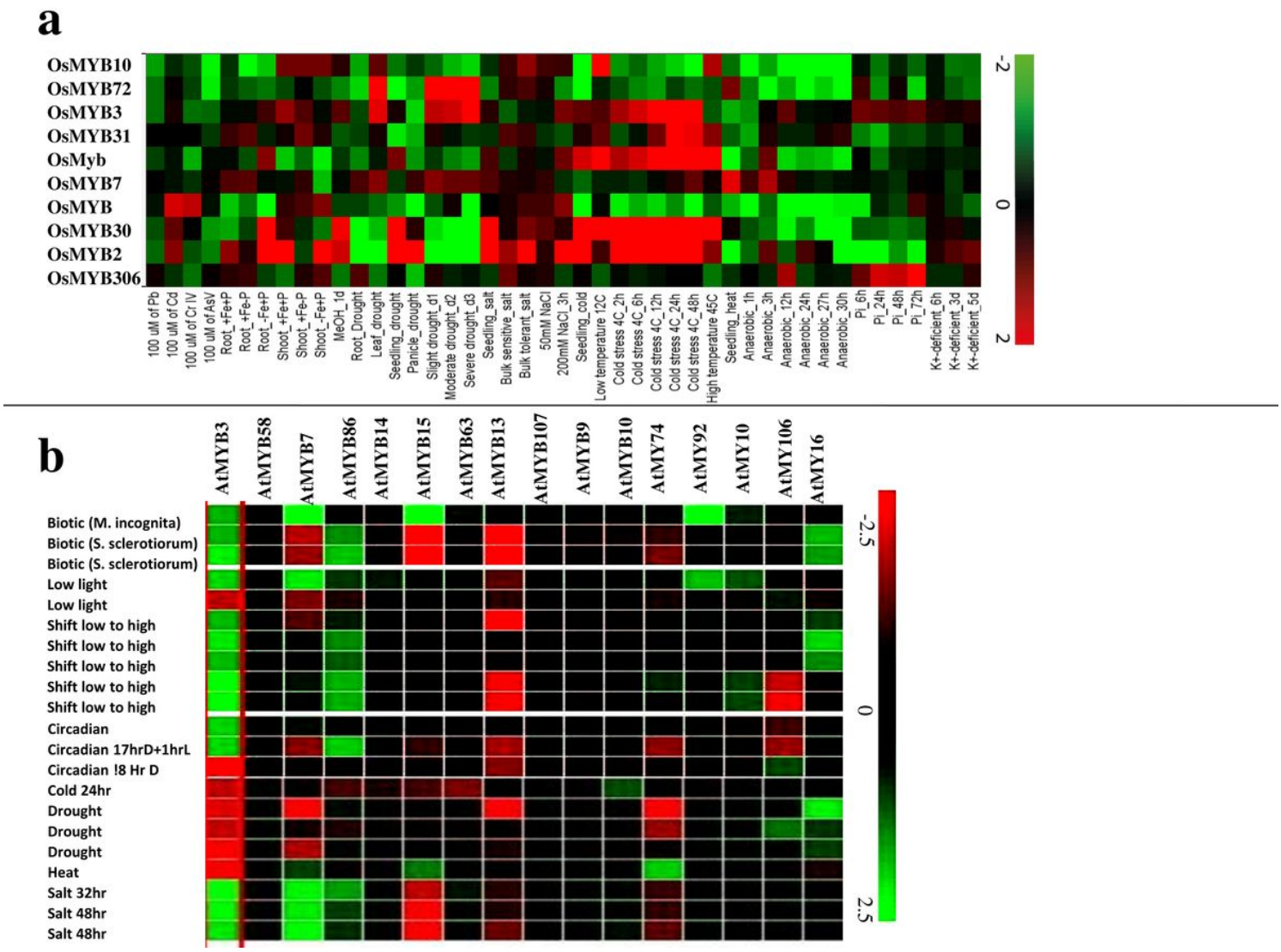


Figure 6

Expression profile of MYB genes under abiotic stress conditions. Heat maps show the microarray-based expression pattern of MYB genes from Rice **(a)** and Arabidopsis **(b)** under conditions of salt, drought and cold as indicated at the bottom of the heat map. Color bars at the bottom of each of the heat maps show the corresponding scale for log2 fold change in expression

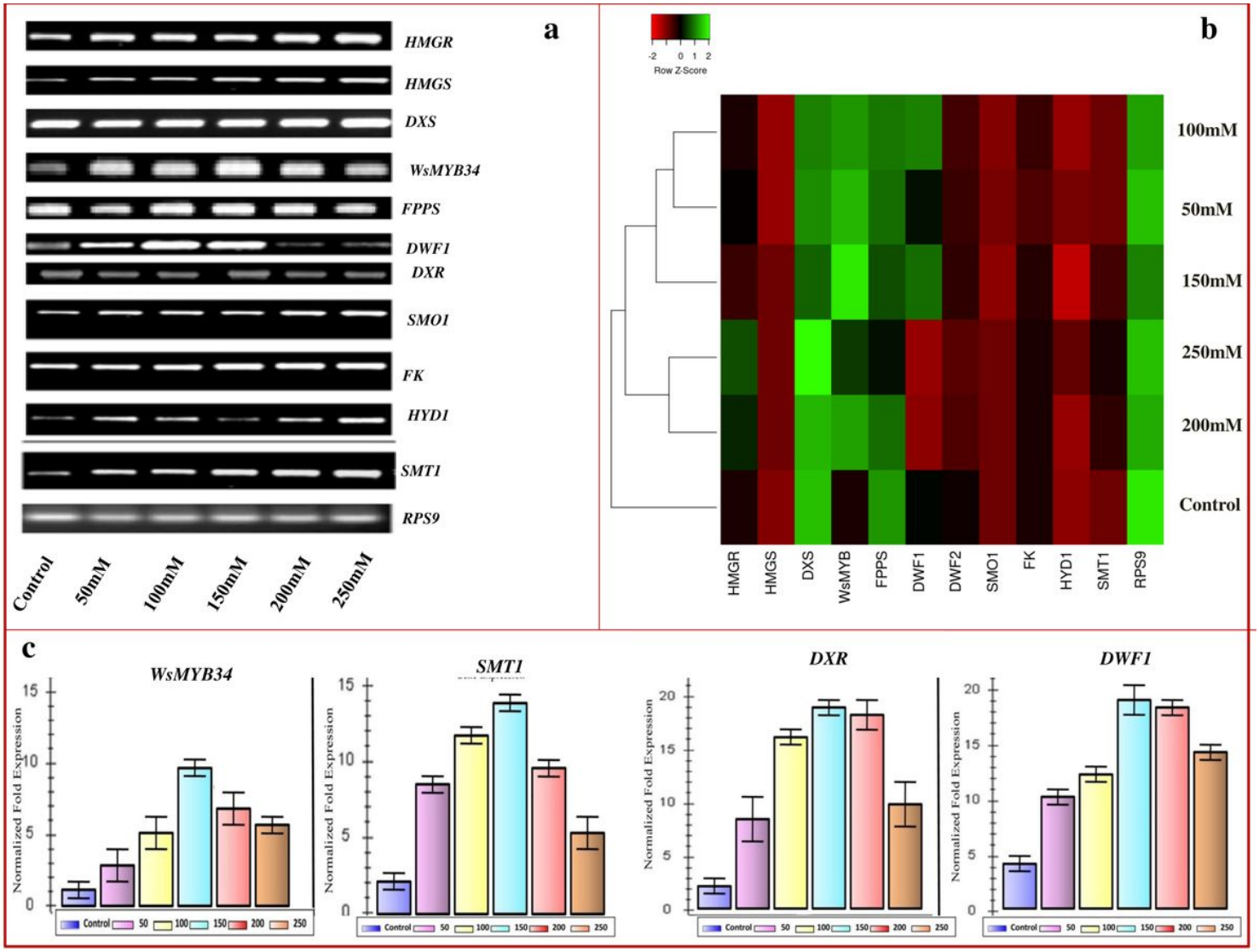


Figure 7

Effect of different concentrations of NaCl on expression analysis of withanolide synthetic and stress responsive genes. (a) Analysis of gene expression pattern by RT-PCR, (b) pictorial representation of relative levels of transcripts in the form of heat-map, and (c) expression analysis of withanolide synthesizing genes and *WsMYB34* gene by real-time PCR. [(HMG-CoA reductase *HMGR*), (HMG-CoA synthase *HMGS*), (1-deoxy-D-xylulose-5-phosphate synthase *DXS*), *WsMYB34*, (farnesyl pyrophosphate synthase *FPPS*), (delta-24 sterol reductase *DWF1*),(sterol delta-7 reductase*DXR*), (C4-methyl sterol oxidase 1 *SMO1*), (delta 14-sterol reductase *FK*), (C-7,8 sterol isomerise *HYD1*), (sterol methyltransferase 1 *SMT1*)]

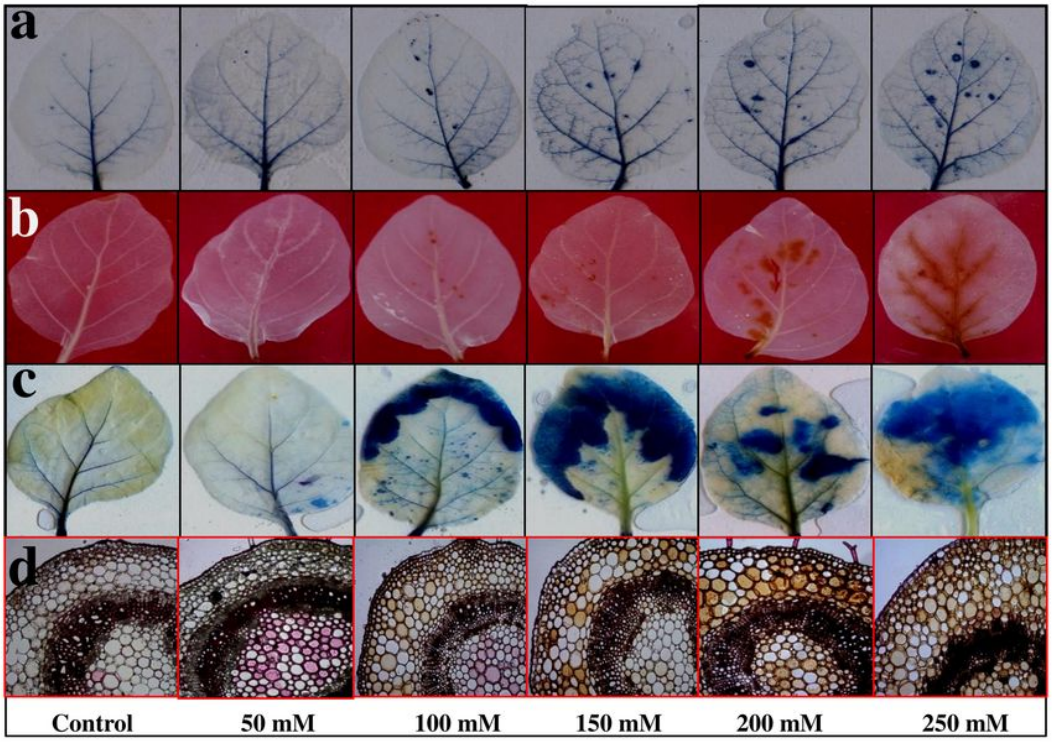


Figure 8

Effect of different concentrations of NaCl on ROS accumulation and cell death of *Withania somnifera.* (a) *in-vivo* histochemical detection of O_2•− radicals by NBT staining; (b) detection of H_2O_2 by DAB staining; (c) assessment off cell death by Evan's blue staining; and (d) assessment of anatomical features of *Withania somnifera.* (E= epidermis, C= cortex, VB= vascular bundle, Pi= pith, T= trichome)

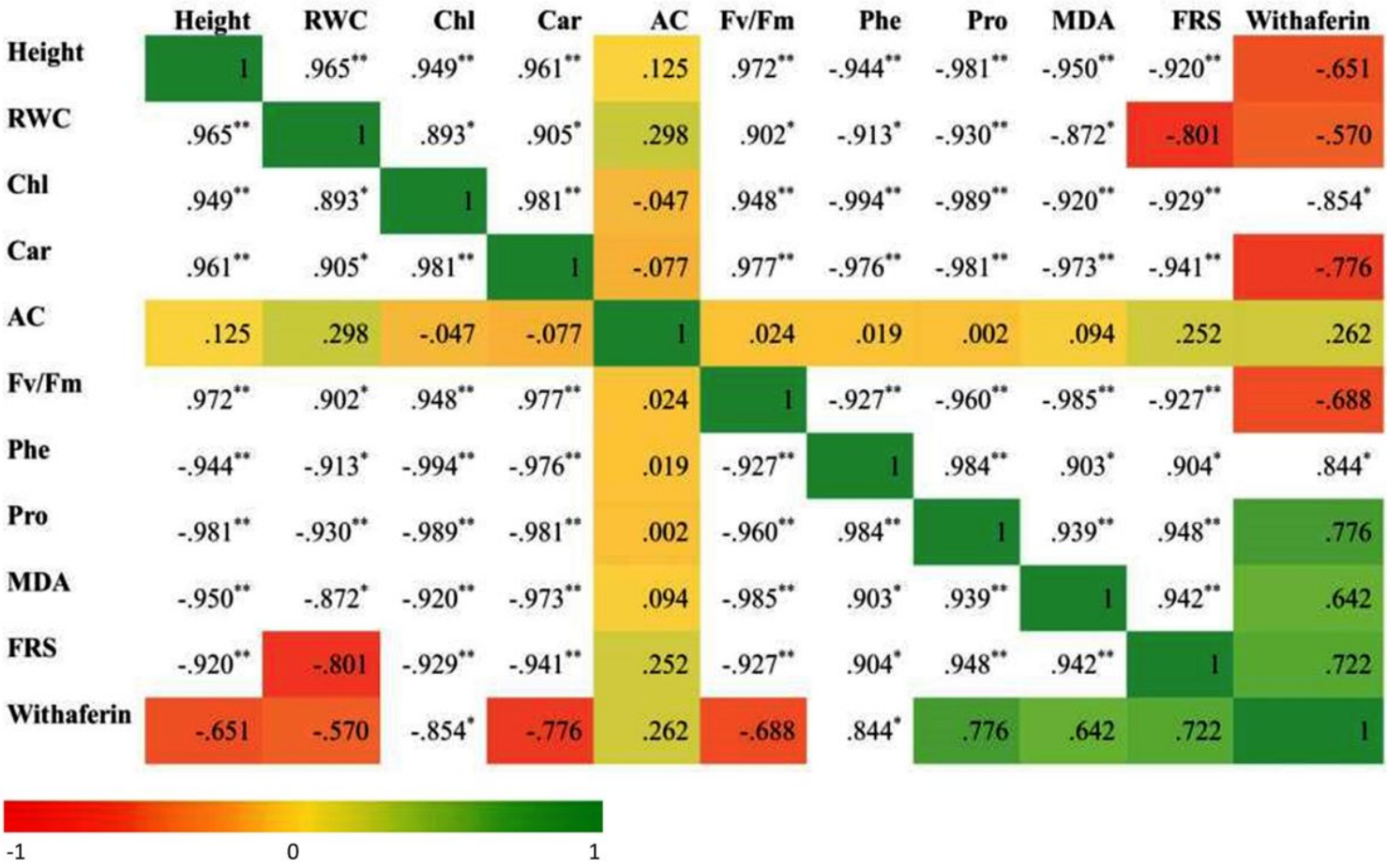


Figure 9

Correlation analyses amongst various morphological, physiological, and biochemical parameters of control and NaCl treated *Withania somnifera*. (RWC: relative water content; Chl: total chlorophyll; Car: carotenoid; AC: anthocyanin; Phe: phenol; Pro: proline; MDA: malondialdehyde; and FRS: Freeradical scavenging activity)

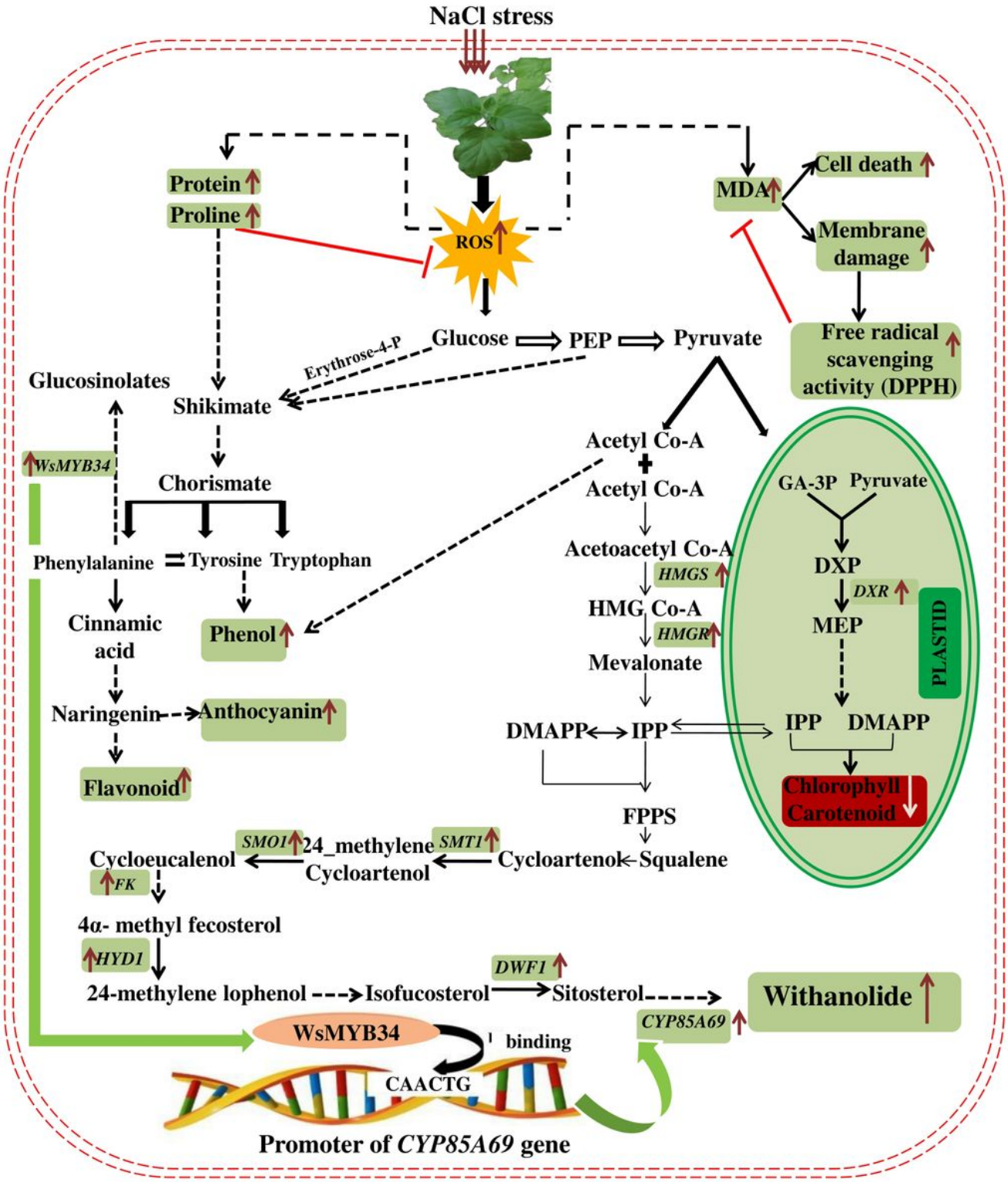


Figure 10

A hypothetical model and pathway to describe the effects of NaCl stress on biochemical and molecular behaviour of *Withania somnifera* as well as regulatory role of WsMYB34 TF in plant metabolism

Supplementary Files

This is a list of supplementary files associated with this preprint. Click to download.

- Supplimentarydata.pdf